CHARACTERIZATION AND MODELING OF NITRIC OXIDE RELEASE IN AQUEOUS SOLUTIONS

By

ANAND RAMAMURTHI

Bachelor of Engineering

Bangalore University

Bangalore, India

1994

Submitted to the Faculty of the
Graduate College of the
Oklahoma State University
in partial fulfillment of
the requirements for
the degree of
MASTER OF SCIENCE
December, 1996

CHARACTERIZATION AND MODELING

OF NITRIC OXIDE RELEASE IN

AQUEOUS SOLUTIONS

Thesis Approved:

Randy S. Lewis

Thesis Adviser

Karen A. High

Gary L. Foutch

Thomas C. Collins

Dean of the Graduate College

ACKNOWLEDGMENT

Respectful thanks are due to my parents, Meena and V. Ramamurthi for their love and support, and for having always guided me along the right path. I dedicate this thesis to them. To my brother Rajkumar, no words of appreciation will suffice for the wonderful moral support he has been to me all these years. A sincere thank you to Dr. Randy S. Lewis for proving to be an inspiration both as an adviser and as an individual. None of this would be possible if not for his encouragement, and the active interest he showed in my research. I am grateful to him and the department of Chemical Engineering for having financially supported me during the period of my graduate studies.

I wish to thank Dr. Gary L. Foutch and Dr. Karen A. High for serving on my thesis committee. Special thanks go to Mr. Charles Baker and the staff of Chemical Engineering for their help and understanding. I would also like to express my appreciation to Shravan, Joseph, Kimberly, Johnny, Mahesh and Sameer for their friendship and for providing a pleasant work environment.

Most important, my respectful prayers are due to God Almighty for having seen me safely through good and bad times, and for having led me to where I am today. I surrender my all to him.

TABLE OF CONTENTS

LIST OF FIGURES

Figure Page

LIST OF TABLES

NOMENCLATURE

k_M	First order rate constant for NONOate decomposition (s^{-1})
E_{NO}	Moles of NO released per mole of NO-donor decomposed
k_1	Rate constant for the aqueous reaction of NO with O_2 (M^{-2} s^{-1})
$(k_L A/V)_x$	Overall volumetric mass transfer coefficient for species 'x' (s^{-1})
$(k_G A_G/V)_{NO}$	Volumetric mass transfer coefficient for NO at the gas-liquid interface (s^{-1})
$(k_B A_B/V)_{NO}$	Volumetric mass transfer coefficient for NO at the base of the stirred cell (s^{-1})
[M]	Aqueous NO-donor concentration (μM)
P_{O2}	Partial pressure of oxygen (MPa)
P_{NO}	Partial pressure of NO (MPa)

CHAPTER 1

INTRODUCTION

Nitric oxide (NO) is a colorless, odorless gas which can be highly toxic. Until the past decade, NO was primarily identified as an industrial air pollutant. It has recently been identified as a biological molecule involved in several physiological and pathophysiological processes. Owing to its free radical structure, the high reactivity of NO is critical for many of its biological roles.

NO is synthesized endogenously by various mammalian cell types including macrophages, neutrophils, endothelial cells, and hepatocytes. Specifically, it is synthesized from the amino acid L-arginine by the nitric oxide synthase (NOS) enzyme. The enzyme is generally classified as constitutive or inducible. The constitutive enzyme is calcium dependent and releases picomolar (10^{-12} M) levels of NO in response to physical receptor stimulation. The NO released plays an important role as a biological messenger, such as in blood pressure regulation. The inducible enzyme is induced by compounds such as cytokines which are released during immunological reactions. The time period of NO release is longer than the constitutive NOS. The NO released is in the nanomolar range and is often toxic towards foreign microorganisms as well as tumor cells and has been associated with tissue damage and excessive vasodilation [Moncada et al., 1994].

1.1 Physiological roles of nitric oxide.

Several physiological roles for NO have been identified using techniques such as inhibition of NO synthesis by introduction of analogues of L-arginine or identification of NO synthesis through biochemical assays.

1.1.1 Role of NO in vascular relaxation.

One of the vital effects of the contraction and expansion of the smooth muscles surrounding blood vessels is the of control of resistance to blood flow (i.e., blood pressure regulation). Naturally occurring mediators, such as acetylcholine, have been shown to act on vascular endothelial cells to release an endothelium derived relaxing factor (EDRF). This factor directly affects neighboring smooth muscle cells, which causes muscle relaxation and vasodilation. *In vitro* studies by Moncada, Palmer and Ferrige (1987) have conclusively shown that EDRF is the NO molecule. NO release is also stimulated from the endothelial cells of the arterial endothelium via shear stress [Butler and Williams, 1993].

1.1.2 Role of NO in platelet aggregation.

Excessive bleeding due to blood vessel damage is prevented by aggregation of granular blood platelets to form a clot. However, abnormal clotting of blood in blood vessels may cause myocardial infarction (heart attack) due to hampered blood supply. NO has been shown to inhibit platelet aggregation thus helping to maintain anti-clotting effects in non-injury regions. The NO is either derived from the vascular

endothelial cells or produced by arginine-activated enzymes within the platelets themselves [Butler and Williams, 1993].

1.1.3 Role of NO in the central nervous system.

Neurotransmitters are chemical messengers which help convey electrical impulses across the gaps between nerve cells. Knowles et al. (1989) identified NO as one of the chemical messengers involved in feedback loop or retrograde neurotransmission. An amino acid neurotransmitter stimulates a postsynaptic neuron to produce NO, which diffuses and acts on the presynaptic neuron to strengthen the connection between the nerve cells. Suggestions have been made that NO plays an important role in blood supply within the brain and has a long term effect on brain development, learning, and memory. This latter role of NO is being utilized in memory research for its viability in treatment of certain neurodegenerative diseases [Moncada et al., 1993].

1.1.4 Role of NO in the endocrine system.

Although studies in this area are yet at a preliminary stage, indications are that NO plays a role in the regulation of renin production and sodium homoeostasis in the kidney. Shear stress across the endothelial cell surface occurs due to enhanced renal blood flow. The stress activates the NOS to synthesize NO, which in turn inhibits release of renin [Vallance and Collier, 1994].

1.1.5 Role of NO in immunological responses.

One method through which macrophages destroy invading microbes and other types of foreign cells is through the release of cytotoxic substances. Response of the macrophages to these microbes is achieved by the presence of chemical mediators called cytokines, which stimulate the macrophages to generate NO. NO can then disable or kill the foreign organisms disabling key enzymes or by other mechanisms which involve the reaction of NO with species such as oxygen or superoxide to form cytotoxic intermediates [Butler and Williams, 1993].

1.2 Pathophysiological roles of NO

The toxicity of NO and its beneficial aspects are likely related to its concentration in the biological system. Normally, endothelial cells generate NO concentrations on the order of picomolars, and macrophages on the order of nanomolar amounts. In situations where overproduction or deficiency of NO occurs, certain pathophysiological disorders can develop. However, some of these may be partly or completely reversed by either scavenging the excess NO or introducing NO through the use of NO releasing drugs [Kerwin et al., 1995]. Pathophysiological effects related to NO may be divided into two general categories - (i) high levels of NO and (ii) low levels of NO.

1.2.1 Effects of high levels of NO.

1.2.1.1 Hypotension /Septic shock.

Following massive infection or injury, macrophages aggregate at the injury site to counteract invading microorganisms. Production of NO by macrophages, due to expression of the inducible form of NOS, has a two-way effect. The first serves the beneficial purpose of eliminating the invading cells via cytotoxic mechanisms. The second effect is adverse, causing substantial vasodilation and subsequent drop in blood pressure which results in septic shock [Kerwin, Lancaster, and Feldman, 1995].

1.2.1.2 Tissue damage associated inflammation.

Nitric oxide is produced upon activation of immune cells following stimulation by bacterial endotoxin or inflammatory mediators such as cytokines [Vallance and Collier, 1994]. Tissue damage may occur due to increased vascular perfusion or by reaction of NO with superoxide to produce peroxinitrite which can promote cell lipid oxidation as well as other damaging effects [Kerwin et al., 1995].

1.2.1.3 Rheumatoid arthritis.

NO has been implicated in the development of rheumatoid arthritis. Inflammatory mediators stimulate the cells of synovial joints, and the leucocytes that infiltrate them during inflammation, to activate inducible NOS which then generates high levels of NO. The

primary effect is increased vasodilation and further swelling of the joints [Evans et al., 1995].

1.2.1.4 Insulin-dependent Diabetes Mellitus.

Pancreatic beta cells secrete insulin to help control glucose metabolism. Cytokines have been identified as immunological effector molecules involved in mediation of beta cell destruction associated with insulin dependent diabetes mellitus. Research by Corbett et al. (1993) has shown that cytokines induce NO formation within islet cells. The overproduced NO causes beta cell dysfunction [Corbett et al., 1993].

1.2.2 Effects of low levels of NO.

1.2.2.1 Pulmonary hypertension.

NO generated by endothelial cells of small arterioles in the lungs helps maintain a basal vasodilator tone. Calver et al. (1992) observed a correlation between impaired NO synthesis and pulmonary hypertension.

1.2.2.2 Artherosclerosis.

One of the effects of an underproduction of endogenous NO is the increased adhesion of macrophages and neutrophils to the endothelium and later formation of foam cells leading to constriction of the area for blood flow. In the presence of lower concentrations of NO, superoxide is not adequately scavenged. The superoxide inhibits endothelial NOS activity leading to decreased synthesis of NO and subsequent lowering of the vasodilation potential and also causes a gradual loss of the basal vasodilator tone [Kerwin et al., 1995].

1.3 Reactivity and cytotoxicity of NO.

Nitric oxide formed in many cells serves several beneficial processes such as interneuronal communication or participation in the functioning of the immunological response system. NO undergoes a number of complex and sequential reactions in an oxygenated biological system. It is often the case that 'NO induced' cytotoxicity is not due to NO alone, but also due to active intermediates or products of the many reactions with NO. NO may not only be cytotoxic to invading microbes following an immunological response, but in many cases it may destroy or modifiy the function of healthy cells in the body. Death or mutagenicity of cells can be caused by DNA damage inflicted by NO or its reaction products.

1.3.1 Reaction of NO with O_2.

Nitric oxide reacts with oxygen according to

$$2\ NO + O_2 \longrightarrow 2\ NO_2 \qquad (1.1)$$

$$NO + NO_2 \longrightarrow N_2O_3 \qquad (1.2)$$

Nitrous anhydride (N_2O_3) can then diassociate in aqueous media to yield nitrite (NO_2^-) [Lewis et al.,1994]

$$N_2O_3 + H_2O \longrightarrow 2\ H^+ + 2\ NO_2^- \qquad (1.3)$$

N_2O_3 can damage DNA via two different pathways. The first pathway is through the nitrosation of secondary amines to form carcinogenic N-Nitrosoamines. In the presence of

appropriate enzyme systems, these form alkylating electrophiles which react with the nucleophilic sites on the DNA strands leading to indirect DNA damage.A second pathway involves direct DNA destruction through nitrosative deamination of primary amines attatched to the DNA bases. This leads to weakening and subsequent breakage of the DNA strands [Tannenbaum et al., 1991].

1.3.2 Reaction of NO with superoxide.

DNA damage or lipid peroxidation can also occur due to species formed from NO reactions or by oxygen free radicals. Beckman et al. (1991) has shown that superoxide (O_2^-) is involved in this cytotoxic mechanism. NO reacts with (O_2^-) to yield peroxynitrite ($ONOO^-$)

$$NO^{\cdot} + O_2^- \longrightarrow ONOO^- \qquad (1.4)$$

Species formed by further reactions of ($ONOO^-$) are toxic, mutagenic or bacteriocidal, and cause destruction of lipid membranes and DNA. This is the phenomenon of oxidative stress associated with reperfusion injury [Hogg et al., 1992].

1.3.3 Reaction of NO with transition metals/ metal groups.

NO reacts with transition metals incorporated in chelate structures. Many proteins such as hemoglobin, myoglobin, and cytochromes contain metal groups. NO can react with these proteins to form metal-nitrosyl complexes. These complexes can release NO under appropriate biological conditions or can act as nitrosating agents through NO donation. Further, the reversible or irreversible binding of NO to a metal group, in an enzyme structure

can lead to distortion of the enzyme and subsequent loss or change in functionality. Certain dioxygenated metal groups such as oxyferrohemoglobin can act as scavengers of NO. NO also reacts with deoxyferrohemoglobin to form a nitrosyl complex which can either be carcinogenic or release NO [Kerwin et al., 1995].

1.4 Development of NO delivery systems.

NO has both harmful and beneficial roles in biological systems. The mechanisms via which NO interacts with biological systems can be understood through *in vitro* studies with cell cultures or *in vivo* studies through the delivery of NO. To effectively study NO effects, a method is required by which known or predictable quantities or concentrations of NO are delivered to the system under study. A second rationale for delivering NO to physiological systems is for the treatment of certain pathophysiological disorders. It is therefore imperative to develop a suitable NO delivery system capable of consistent and predictable NO delivery rates. Generally, there are two different approaches.

1.4.1 Physical method.

The physical method involves NO delivery from the gaseous phase, via diffusion through a semi-permeable membrane, to an aqueous solution. This method has been used to determine the influence of delivery rate of NO on the biological effects of several cellular systems [Tamir et al., 1994]. The delivery of NO to an aqueous solution could be regulated

by changing parameters such as the partial pressure of the gas and the length of the semipermeable membrane.

1.4.2 Chemical method.

The chemical method involves dissolution of an NO releasing compound. Nitric oxide is a generated moiety of glyceryl trinitrate and other nitrovasodilator compounds, which helps to counteract the effects of hypertension [Vallance and Collier, 1994]. Nitric oxide donors such as amyl nitrite have been used in the past for treatment of asthma by inducing vasodilatation [Riegel, 1876]. A number of NO donors are available commercially which differ in their properties and NO release characteristics. These include :

(i) SIN-1 : A morpholine based NO donor which releases both NO and O_2^-.

(ii) Molsidomine : An orally active NO donor which releases NO in response to specific hepatic metabolic processes.

(iii) NONOates : Nucleophile/ NO adducts which generate NO following pH dependent decomposition.

1.5 General thesis objective

The primary objective of the thesis is to determine the precise kinetics and time dependent NO release characteristics of specific NO chemical donors and to estimate the NO concentrations or delivery rates to the system of study. Nitric oxide donors can be used to deliver NO to NO-deficient biological systems for therapeutic purposes, or to study the biological roles of NO. However, predictable NO delivery is essential since various

amounts of NO can have different biological effects. The predictability is important when seeking to avoid unwanted or toxic reactions with other species present in the system under study. Proper characterization of the NO donors for the elucidation of their kinetics of NO release will help in the design of methods for NO therapeutic applications and in the quantitative study of NO with regards to its biological role.

CHAPTER 2

CHEMICAL METHODS OF NITRIC OXIDE DELIVERY

Several compounds such as SIN-1, Molsidomine and NONOates are capable of generating NO upon dissolution in aqueous solutions. Such NO donors have a good potential as research tools or for incorporation as drugs to deliver predictable quantities of NO to targeted areas. One of the recently developed classes of NO donors are the NONOates which have a general structure $XN(O^-)N=O$. These compounds are formed by the reaction of a nucleophile with NO. The binding of NO and the nucleophile takes place via a nitrogen atom (as primary, secondary or polyamines), an oxygen atom (as an oxide) or a sulfur atom (as a sulfite). Commercially available NONOates which have different nucleophilic residues include Spermine, Diethylamine, PAPA, DETA, and MAHMA NONOates. Accordingly, they exhibit different NO release characteristics with regards to the NONOate decomposition rate constant (k_M) and the number of moles of NO released per mole of the NONOate decomposed (E_{NO}).

2.1 Basis for NONOates as NO delivery compounds.

NONOates have several benefits for the delivery of NO. These include :

a) NONOates exhibit first order release kinetics.

b) Several NONOates are commercially available, exhibiting a wide variation in

their NO release characteristics. This allows for selection of the donor compound based on specific requirements.

c) NONOates are stable as solids which allows them to be stored for up to 6 months under inert atmospheric conditions at -80 °C.

d) NONOates do not decay in alkaline solution, which allows for administration of NONOates in a liquid medium.

2.2 Previous NONOate studies.

The pioneering work of NONOate synthesis and characterization was done by Maragos and co-workers [Maragos et al., 1991]. In one study, five different NONOate species were characterized. NONOate decomposition was characterized using first order kinetics according to the following reaction :

$$XN(O^-)N{=}O \xrightarrow{k_M} X^- + 2(NO) \qquad (2.1)$$

where k_M is the rate constant for the first order decomposition. E_{NO} was defined as

$$E_{NO} = \frac{\text{Moles of NO generated}}{\text{Moles of NO-donor decomposed}} \qquad (2.2)$$

Theoretically, for NONOates, E_{NO} is 2.

The method for characterizing the NONOates took into account the properties of NONOates. The properties of two commercially available NONOates are shown in Table I. In general, NONOates are stable as solids (in an inert Ar/N_2 atmosphere) or in solution at high pH (pH > 12.0) but decompose to release NO when dissolved in solutions at a lower pH.

TABLE I

PROPERTIES OF SPERMINE AND DIETHYLAMINE NONOATES

Property	Spermine NONOate	Diethylamine NONOate
Nucleophilic residue	Zwitterion	Secondary amine
Formula wt.	262.4	206.3
Molecular Formula	$C_{10}H_{26}O_2$	$C_4H_{10}N_3O_2.C_4H_{12}N$
Indicated purity	>98 %	>98 %
Appearance	White crystalline powder	Off-white crystalline powder
Sensitivity to oxygen	Yes	Yes
Storage	-80°C (under argon atmosphere)	-80°C (under argon atmosphere)
Stability	Solution of NONOate in 0.01 M NaOH @ 0°C for 24 hours	Solution of NONOate in 0.01 M NaOH @ 0°C for 24 hours
Maximum absorbance	UV @ λ = 250 nm	UV @ λ = 250 nm
Emissivity	8000 au/M	6500 au/M

A thermostatic reactor maintained at physiological temperature (37 °C) was purged with inert helium gas to remove reactive species such as oxygen and NO that may have been present initially. Following this, the NONOate (dissolved in alkaline buffer) was introduced into the reactor. Deoxygenated phosphate buffer (pH 7.4) was then injected into the reactor through an air-tight septum to initiate NONOate decomposition and NO generation. The generated NO was purged from the aqueous phase into the gas phase using helium. The NO/Helium mixture was sent to a chemiluminescence detector where the NO was quantified.

2.2.1 Determination of E_{NO}

Maragos and co-workers (1991) determined E_{NO} from the gas phase NO detector response curve after complete decomposition of the NONOate. The area under the response curve represented the number of moles of NO generated from the NONOate, based on the calibration of the chemiluminescence detector. The number of moles of NONOate decomposed was based on injection amounts.

The average E_{NO} value was 1.90 ± 0.00 (*sic*) for Spermine NONOate at pH 2.0 and 1.50 ± 0.11 for Diethylamine NONOate at pH 7.4. E_{NO} values for other NONOates were also determined, but were much lower than the theoretical limit of 2.0 (values ranged from 0.001 to 0.73). It was also noted that E_{NO} was enhanced by increasing the acidity of the aqueous medium. One drawback of this procedure was that the determination of E_{NO} necessitated the complete decomposition of the NONOate. In view of the slow decomposition rate observed for Spermine NONOate (observed $t_{1/2}$ = 39 min.), it was

necessary to carry out characterization at a much lower pH of 2.0, to ensure complete decomposition within a reasonable experimental time.

2.2.2 Determination of k_M

The NONOates have characteristic UV absorbances at specific wavelengths (e.g., λ = 252 nm for Spermine NONOate and λ = 250 nm for Diethylamine NONOate). This allowed for quantitation of these complexes in aqueous solutions. As the decomposition proceeded, gradual loss of the intense initial chromophore occurred leading to a drop in the absorbance. The decaying absorbance was used to determine the first order rate constant k_M. The rate expression for the first order decomposition of the NONOate is

$$\frac{d[XN_2O_2]}{dt} = -k_M[XN_2O_2] \qquad (2.3)$$

Integrating with time yields

$$(XN_2O_2) = (XN_2O_2)_o\, e^{-k_M t} \qquad (2.4)$$

where $(XN_2O_2)_o$ refers to the initially charged NONOate concentration. Since absorbances were proportional to the aqueous NONOate concentration, concentrations in Eq. 2.4 could be replaced with absorbances. A plot of $-\ln[(abs)/(abs_o)]$ versus time would yield a slope of value k_M.

The absorbance versus time profile was observed to be an exponential decrease, thus confirming the use of the above equation. The value of k_M at 37 °C for Spermine

NONOate and Diethylamine NONOate were $3.0 \pm 0.2 \times 10^{-4}$ s^{-1} and $54.0 \pm 2.0 \times 10^{-4}$ s^{-1}, respectively. Rate constants were sensitive to pH, with decomposition rates increasing with increasing acidity of the aqueous medium.

2.3 Thesis objectives.

Previous efforts in characterizing NONOates had several drawbacks which include the following :

a) Aqueous NO concentrations were not measured. Thus, aqueous NO concentration predictions based on NONOate dissolution kinetics were not validated. This validation would be important when seeking to quantitate NO concentration effects on biological systems, when using NONOate compounds for NO delivery.

b) The method of determining E_{NO} required the complete decomposition of NONOate. Therefore, time constraints did not permit the characterization of Spermine NONOate at physiological pH, but only at pH 2.0. In addition, it was not verified if E_{NO} is constant throughout the NONOate decomposition.

c) The reactions of NO in aqueous media were not monitored. The possibility exists of the generated NO reacting with residual oxygen to form nitrate (NO_3^-) or nitrite (NO_2^-). Reactions in solution would lower the experimental value of E_{NO} if reaction products were not taken into account.

The major thesis objective is to improve the previous methods for NONOate characterization and to validate NO concentration predictions in aqueous solutions

following NONOate decomposition. In addition the methods described are to be general enough to be applicable to other NO-donors utilized in a variety of experimental systems.

Spermine (a polyamine) and Diethylamine (a secondary amine) NONOates were chosen for the study. The structures of these NO donors are shown in Figure 1. These NONOates were chosen since

a) they were shown to release NO amounts close to the theoretical limit of 2 moles of NO per mole of the NONOate decomposed. However, Spermine NONOate was not evaluated at physiological pH [Maragos et al., 1991].
b) they generate high levels of NO as compared to other NONOates, which enables easier and more precise detection of NO.
c) their decomposition rates were observed to differ significantly from each other.

The objective was attained by the completion of the following aims.

2.3.1 Aim # 1 : Measurement of E_{NO} and k_M.

The kinetic parameters for NO release by NONOates were determined as a function of time. Aqueous NO concentrations were measured directly via chemiluminescence, facilitating characterization of the NONOates over shorter periods of time (~2 hours) at physiological pH. Loss of NO from solution through mass transfer was accounted for by determination of the volumetric mass transfer coefficient for NO. Reaction of NO was rendered insignificant by maintaining an oxygen free environment.

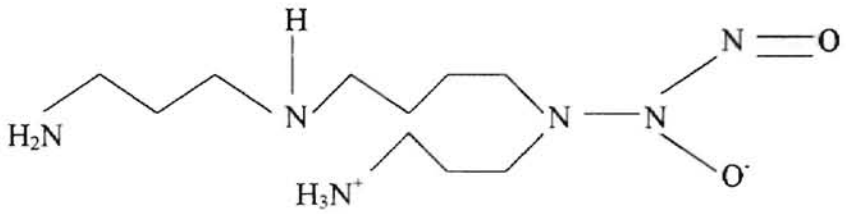

(a)

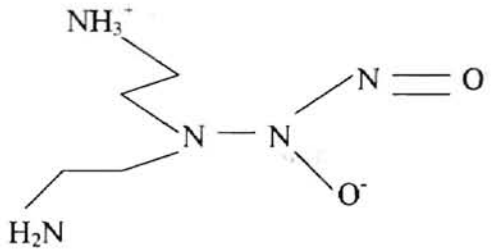

(b)

Figure 1. Molecular structure of Spermine NONOate (a) and Diethylamine NONOate (b).

2.3.2 Aim # 2 : Validation of NO concentrations in phosphate buffer.

A model incorporating the E_{NO} and k_M values was developed. This model would predict aqueous NO concentrations generated over time in oxygen-rich phosphate buffer, following injection of theoretical quantities of NONOates. The model takes into account the depletion of NO in solution by mass transfer and reaction. The model results were compared with direct measurements of aqueous NO concentrations generated by the NONOates.

2.3.3 Aim # 3 : Validation of NO concentrations in other physiological solutions.

The model developed in Aim #2 was utilized to predict aqueous NO concentrations and compare them with NO concentrations experimentally measured in physiological media such as culture medium or Tyrode's solution. The solutions were oxygen saturated. Validity of the model for making reliable predictions would be valuable towards developing other models to enable accurate estimation of aqueous NO concentrations obtained by delivery of theoretical quantities of NONOates to biological systems.

CHAPTER 3

NITRIC OXIDE AND OXYGEN ANALYSIS IN AQUEOUS SOLUTIONS

One of the primary features of the current study is the direct measurement of aqueous NO concentrations, as opposed to the gas phase NO concentration measurements adopted by Maragos et al. (1991). Aqueous NO concentrations can be measured by any of the following methods [Archer, 1993] :

a) Measurement of nitrite (NO_2^-) and nitrate (NO_3^-) formed by the sequential reactions of NO with dissolved oxygen. Detection limits are $\sim 10^{-8}$ M.

b) Detection of adducts formed by the entrapment of NO with nitroso or reduced hemoglobin via electron paramagnetic resonance. Detection threshold is ~ 1 nmol.

c) Oxidation of reduced hemoglobin by NO to methemoglobin which is subsequently detected spectrophotometrically. The detection threshold is ~ 1 nmol.

d) Quantitation of luminescence produced by the gas phase reaction of NO with ozone (Chemiluminescence). The detection limit is 20 pmol for NO in the gas phase.

e) Direct quantitation of NO by an electrode sensor. The detection limit is 1 nM

Drawbacks of several of the above methods include sample preparation problems, potential side reactions and, in the case of the electrode, unreliability under certain experimental conditions.

In the present study, aqueous NO is detected via chemiluminescence. The NO detection method was selected on the basis of the sensitivity and versatility of the technique as well as its proven reliability. The assay is specific for NO, eliminating any contribution to the response due to the presence of other volatile species in the system. The detector used in this study (specified signal to noise ratio is 3:1) has been determined to have a lower detection limit of 0.03 μM.

For detection of aqueous NO concentrations, the original method using chemiluminescence involved stripping the NO from solution by bubbling an inert gas [Archer, 1993]. The gas-phase mixture was then subject to the chemiluminescence assay. The assay takes advantage of the low solubility of NO in the aqueous phase. Disadvantages of this method include the necessity of bubbling (not beneficial for protein solutions), gas-phase rather than aqueous-phase detection and the difficulty in obtaining real-time measurements. In light of the difficulties for making accurate aqueous NO measurements via the stripping technique, the present study incorporated a few modifications. These modifications enabled real-time analysis of the aqueous NO concentration

3.1 Description of experimental setup.

The basis of the experimental design is the application of a semi-permeable membrane which separates the aqueous NO sample from the chemiluminescence detector. With the detector side exposed to vacuum, NO diffuses through the membrane and enters the chemiliminescence detector in the gaseous state.

3.1.1 Design of stirred ultrafiltration cell.

A modified 200 ml ultrafiltration cell [Amicon Inc., Beverly, MA, Model 8200], as shown in Figure 2, was used for this study (see Lewis and Deen, 1994). High speed stirring was achieved using a Corning® magnetic stirrer (model PC-353) and a caged magnetic stirbar. For experiments involving protein solutions which denature by rapid agitation (e.g., culture media), a slow-speed stirrer [Wheton instruments, Milleville, NJ, Model 902400] and a stirrer from a Cytostir® stirred bioreactor (Kontes, Vineland, NJ) were used.

The cell has a stainless steel base with a 1/8" (O.D) stainless steel tubing connected to the detector. The base of the cell incorporates a circular semi-permeable membrane [MEM-100®, Membrane Products, Albany, NY] attached to a Teflon sheet for support. The Teflon sheet has 24 symmetrically punched holes providing a total surface area of 6.788 cm^2 for mass transfer of NO across the membrane and into the chemiluminescence detector [Seivers Instruments, Boulder, CO, Model NOA 270B]. The Teflon sheet limits the area for NO transfer from the solution to the detector and also provides support to the membrane. A thin wire mesh contained in the base provides additional membrane support and also provides volume for vacuum development under the composite membrane.

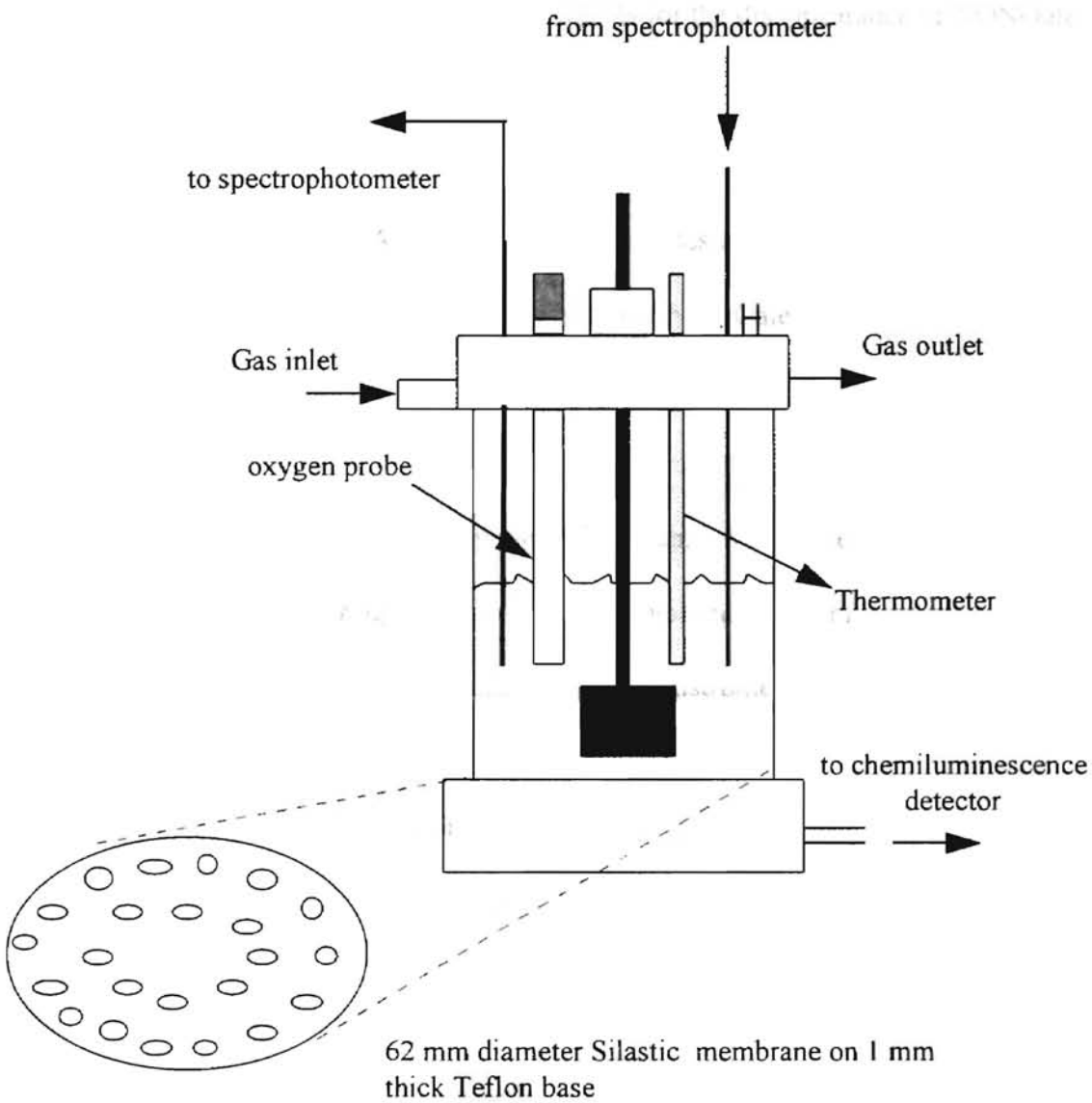

Figure 2. Schematic diagram of the modified ultrafiltration cell

The cell is fitted with a lid containing inlet and outlet ports for gas purging. Two ports are also provided for the inlet and outlet ends of a flow loop. The flow loop is required to spectrophotometrically monitor the vessel contents for the disappearance of NONOate compounds. A septum port is included for introduction of either liquid or gas into the solution. A thermometer and an opening for insertion of an oxygen probe (whenever necessary) are also included. A salient feature of this design is that it permits simultaneous and continuous monitoring of NO, and NONOate compounds.

3.1.2 Flow residence time.

The flow loop incorporated a gear pump [Micropump, Vancouver, WA, Model 000-305]. Liquid was passed through a micro flow cell (volume = 0.3 ml, 10 mm optical path) set in a UV-spectrophotometer (Shimadzu Scientific Instruments, Columbia, MD; Model UV 1601-PC). Teflon tubing (1/8" O.D) was used for the flow loop. The length and diameter of the tubing were selected to minimize the residence time of the fluid within the loop. Two important requirements of the flow loop were :

a) The flow path was to be short such that the residence time of fluid would be negligible. This would minimize time lag during kinetic experiments.
b) A short flow path would avoid rapid cooling down of the circulating fluid, thus maintaining thermal homogeneity of the liquid contents of the system.

The flow rate of fluid through the loop was maintained at 70 ml /min. The loop had a volume of 12 ml. Accordingly, the residence time of a liquid sample within the loop is ~ 10 seconds. This was negligible when compared to the fastest observed NONOate decomposition rates with a half-life on the order of 39 minutes for Spermine NONOate and 2.1 minutes for Diethylamine NONOate. The flow rate maintained was thus deemed appropriate for making real-time spectrophotometric measurements.

3.2 Determination of volumetric mass transfer coefficient.

3.2.1 Importance.

Whether NO is bubbled through the solution contained in the vessel (i.e. NO calibration) or is generated by some species within the solution, mass transfer of NO (or O_2) to or from the solution takes place. Quantitation of the amount of NO transported from solution is important for the analysis of NO generated from NONOates. Lewis and Deen (1994) determined the volumetric mass-transfer coefficients for both NO and O_2 for a similar experimental system. The volumetric coefficients, $(k_L A/V)_x$, are dependent on the liquid volume (V) and the surface area available for mass transfer (A). There are two surfaces across which mass transfer of NO or O_2 takes place to and from the liquid. The first surface across which mass transport occurs is the gas-liquid interface and the second is across the membrane at the bottom of the vessel.

Determination of the NO mass transfer coefficient is necessary to quantify this loss. The protocol for the determination of the NO volumetric mass transfer coefficient is described in the following section.

3.2.2 Experimental protocol.

Initially, 80 ml of deionized water was added to the vessel at 37 °C. The flow loop (12 ml) was also filled with water. The gas phase was then purged with N_2 for a minimum of 45 minutes to remove O_2. Following O_2 purging, a NO/N_2 mixture was introduced into the headspace. Transport of NO into the aqueous solution resulted in an increase in the aqueous NO concentration as detected by chemiluminescence. After the NO concentration was approximately 1 μM, the NO supply was shut off while the N_2 was continuously purged through the headspace. NO in solution depleted through transport into the gas phase and into the detector The NO decay curve was analyzed to determine the mass transfer coefficient. The maximum NO concentration added to the vessel was always less than 1 μM to minimize the potential reaction of NO with residual O_2.

3.2.3 Results.

An NO balance over the contents of the stirred cell gives

$$\frac{d[NO]}{dt} = -4k[NO]^2[O_2] - \left(\frac{k_G A_G}{V}\right)_{NO}\left[[NO]-[NO]^*\right] - \left(\frac{k_B A_B}{V}\right)_{NO}[NO] \qquad (3.1)$$

(a) (b) (c)

where (a) represents the NO consumed by reaction with O_2 and (b) and (c) represent the NO leaving the system at the gas-liquid interface and through the membrane at the base, respectively. The subscripts G and B refer to the gas-liquid interface and the membrane base, respectively. The aqueous NO concentration in equilibrium with the gas phase NO is represented as $[NO]^*$. Purging of the headspace with an inert gas ensures that $[O_2]$ is negligible for significant reaction to take place. In addition, $[NO]^*$ is zero. Thus, equation 3.1 reduces to

$$\frac{d[NO]}{dt} = -\left(\frac{k_L A}{V}\right)_{NO} [NO] \tag{3.2}$$

where the overall mass transfer coefficient $(k_L A/V)_{NO}$ is the sum of $(k_G A_G/V)_{NO}$ and $(k_B A_B/V)_{NO}$. Integration of Eq. 3.2 gives

$$-\ln\left[\frac{[NO]}{[NO]_o}\right] = \left(\frac{k_L A}{V}\right)_{NO} t \tag{3.3}$$

where $[NO]_o$ is the aqueous NO concentration at the initial time. Thus, a plot of $-\ln[NO/NO_o]$ versus time yields a slope of the overall mass transfer coefficient.

The mass transfer coefficient was found to be dependent on the stir speed, geometry of the stirrer and the temperature. The average $(k_L A/V)_{NO}$ was determined for two different experimental setups as shown in Table II.

TABLE II

MASS TRANSFER COEFFICIENT OF NO

Stirrer type	Stir speed (rpm)	Total volume (ml)	$(k_L A/V)_{NO}$ (10^{-4}) s^{-1}
caged stirbar	930	92	48.0 ± 2.1
polysulfone stirbar	85	92	16.8 ± 0.2

In both cases, the mass transfer area was the same. Studies using the polysulfone stirbar did not incorporate the flow loop. However, 92 ml (instead of 80 ml as in caged stirbar study) was added to the vessel.

3.2.4 Effect of metabisulfite.

Initially, an oxygen probe was inserted into the vessel to monitor the O_2 concentration during the course of the experiment. When not in use, the probe was immersed in 2 % sodium metabisulfite to maintain an oxygen-free solution. In spite of repeated washings before use, NO depleted at non-repeatable rates in solution, yielding apparent mass transfer coefficients 1-3 times the values reported above. In addition, an unexplained flattening of the exponential NO decay curve occurred as it approached the baseline. A typical effect of NO loss in the presence of the O_2 probe is shown in Figure 3. Removal of the oxygen probe avoided this problem. Apparently, metabisulfite appears to scavenge NO directly

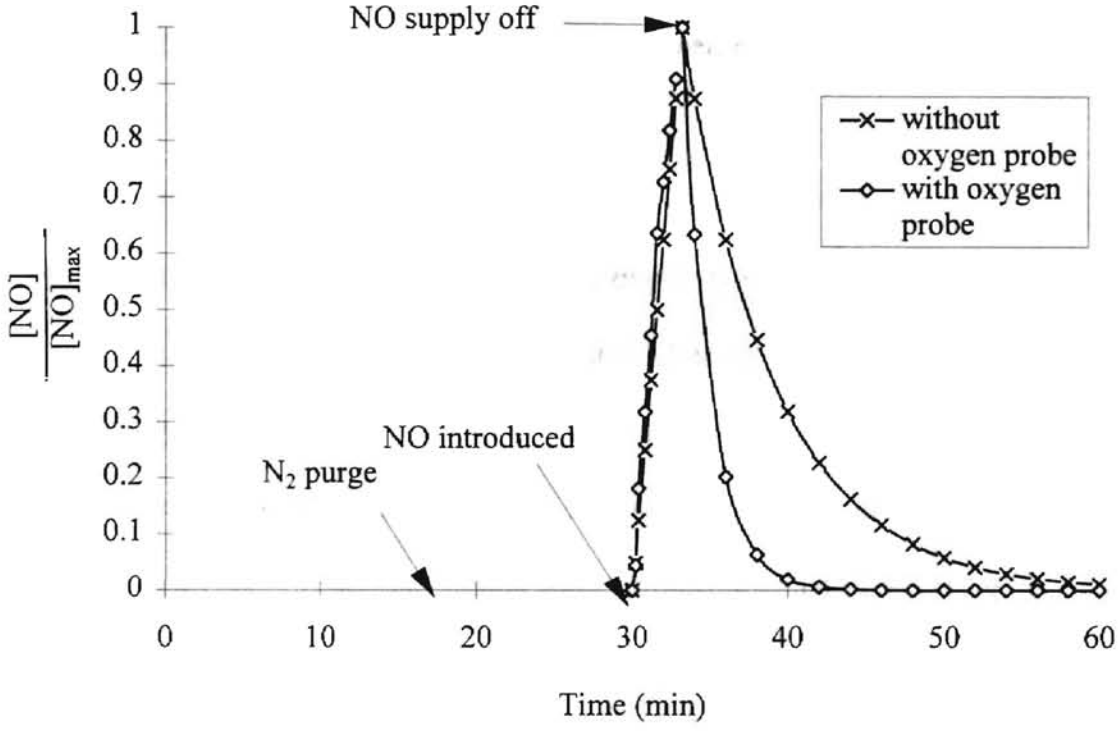

Figure 3. Effect of O_2 probe on aqueous NO depletion.

3.3 Aqueous oxygen concentrations.

During an experiment, aqueous NO can react with dissolved O_2 to form NO_2^-. Thus, O_2 measurements were measured for various protocols using a 12 mm polarographic dissolved oxygen electrode [Phoenix Electrode Company, Houston, TX; Model 025IP-26] connected to an amplifier [Cole-Parmer, Model 01971-00].

3.3.1 Oxygen calibration.

Prior to oxygen calibration, the electrode was zeroed by immersing it in a 2 % (w/v) sodium metabisulfite solution, which provided an O_2-free environment. The O_2 probe was then thoroughly washed and inserted into the liquid in the vessel. The aqueous phase was saturated with air by bubbling air through the solution while maintaining the temperature at 37 °C with uniform stirring. The purging was continued for an hour to ensure saturation. The probe was calibrated at the O_2 saturation value which is $0.0108 \times P_{O2}$ at 37 °C, when the O_2 partial pressure is in MPa [Lange, 1967].

3.3.2 Experimental oxygen concentrations.

Following calibration, the O_2 concentrations were determined for two different experimental protocols. To determine the O_2 concentration during the NONOate characterization studies (see Chapter 4), the saturated solution was depleted of O_2 by purging N_2 through the headspace. Preliminary studies showed that purging the headspace with N_2 was effective in reducing the O_2 concentration levels to less than 3 %

of the saturation value. To determine the O_2 concentration for oxygenated-NONOate studies (see Chapter 5), a saturated O_2 concentration (230 μM at 37 °C) was obtained by bubbling air through the solution for an hour. The bubbling of air into the solution was then stopped and the headspace was continually purged with air, resulting in a slight depletion of O_2 from the solution. This was a result of mass transfer across the gas-liquid interface and through the composite membrane at the bottom of the stirred vessel. The steady-state dissolved O_2 was 87 % of saturation. The O_2 probe was not used in the NONOate experiments because of the difficulty in removing metabisulfite from the probe following storage. Indications from preliminary experiments were that NO reacted with metabisulfite affecting NO concentration readings.

3.4 Calibration of aqueous NO.

Prior to experiments involving NO detection, it is imperative to calibrate the detector response using known aqueous NO concentrations.

3.4.1 Protocol

The phosphate buffer at 37°C (0.1 M, 92 ml) was bubbled in the vessel for approximately one hour with high purity N_2 to remove O_2. NO was then added to the N_2 stream. The NO partial pressure in the gas stream was adjusted using mass flow controllers [Porter Instrument Co., Hatfield, PA]. The gas mixture was passed through a column of soda lime to remove traces of NO_2. Bubbling was continued at a specific NO partial pressure until the aqueous NO concentration achieved steady state. The detector

response was recorded using a chart recorder. Figure 4 shows a typical response of the chemiluminescence detector during the calibration. The NO concentrations were calculated from solubility data. At 37 °C, the aqueous NO concentration (in μM) is 0.0162 x P_{NO} with the NO partial pressure in MPa [Lange, 1967].

3.4.2 Calibration results

Calibration of the detector response indicated that over the expected range of operation (0.1-10 μM NO), the relationship of detector response to the aqueous NO concentration was linear. Figure 5 shows a typical calibration curve. The detection limit is ~ 0.03 μM. Calibrations were done each day in which experiments were performed.

3.5 Conclusions.

The modified stirred ultrafiltration cell adopted in this study is convenient for the measurement of aqueous NO concentrations through chemiluminescence detection. The design of the apparatus provides the following advantages :

a) It is easily fabricated.

b) Mass transfer through the base can be easily manipulated by changing the membrane area available for mass transfer.

c) High chemiluminescence sensitivity to NO requires removal of only minute quantities of NO from solution for detection.

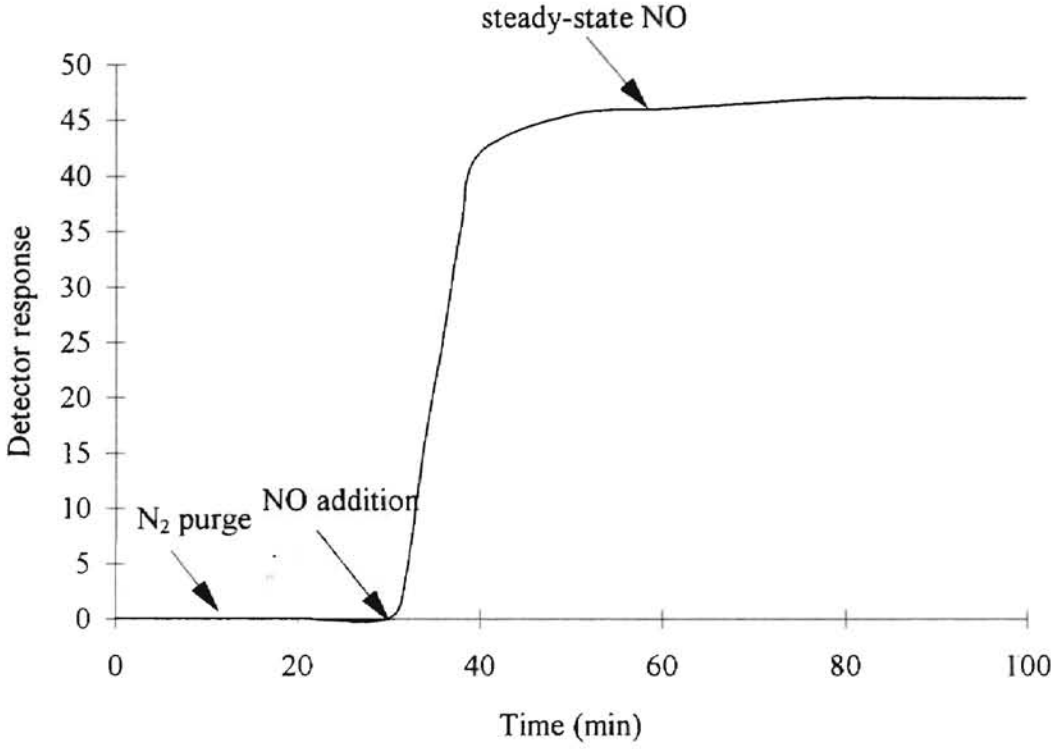

Figure 4. Chemiluminescence detector response during calibration. Detector Response is represented in terms of grapher units.

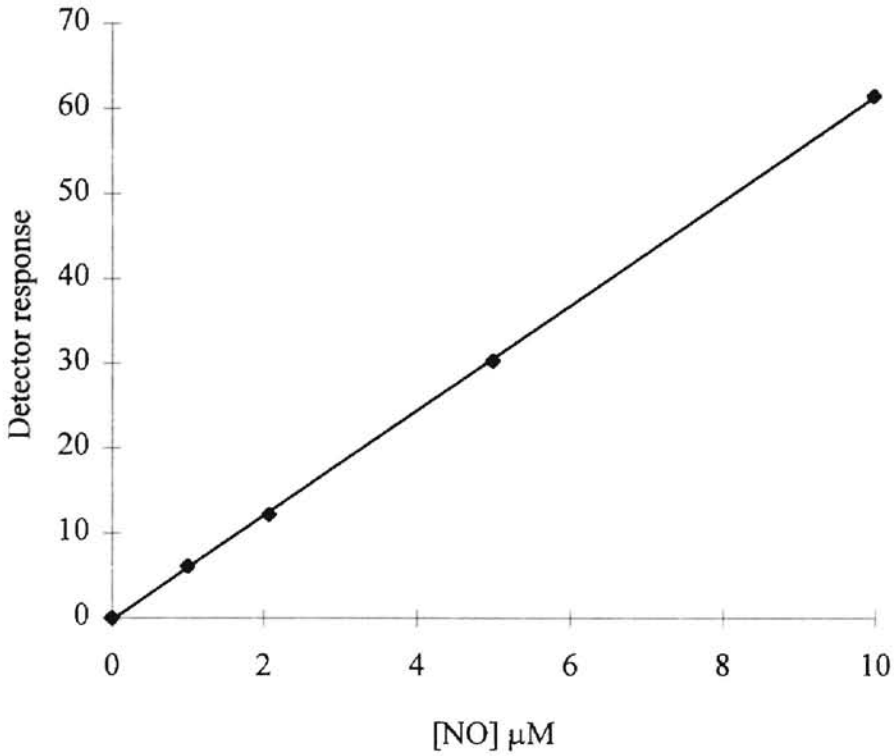

Figure 5. Detector calibration.

d) The design enables simultaneous measurement of aqueous NO concentrations as well as quantification of NO_2^- and NONOate compounds using spectrophotometric detection.

Preliminary experiments showed that dissolved O_2 in the system can be depleted to less than 3 % of the saturation value, following purging with N_2. Achievement of an oxygen- free system would minimize the depletion of aqueous NO via reaction with O_2.

CHAPTER 4

CHARACTERIZATION OF NONOATES

The chemical method of NO delivery described in section 1.4.2 involves NO generation by dissolution of NO generating compounds in aqueous solutions. NONOates are one class of NO generating compounds. Prior to any therapeutic or research applications for which NONOates may be utilized, it is important to determine their NO release characteristics and the kinetic parameters E_{NO} and k_M. Knowledge of these parameters facilitates the development of a model capable of aqueous NO concentration predictions.

The features of the NONOate characterization procedure adopted in the current study, as compared to previous studies [Maragos et al., 1991], include :

a) Accounting for the loss of NO from solution through mass transfer across the gas-liquid interface and membrane at the base.
b) Minimization of NO consumption by reaction with O_2 such that the reaction is justifiably neglected in the analysis.
c) Direct measurement of aqueous NO concentration.
d) Determination of the time dependence of E_{NO}.

Characterization was carried out at physiological pH (pH 7.4) and 37 °C.

4.1 Experimental method.

The experimental protocol for the characterization of Spermine NONOate and Diethylamine NONOate was as follows.

4.1.1 Protocol.

Due to the stability of NONOates at high pH, the NONOate sample was prepared by dissolution of 10 mg of NONOate in deoxygenated pH 12.0 solution (0.1 M NaOH + 0.1 M Sodium diphosphate). Deoxygenation of the solution was achieved by purging with N_2 for 30 minutes. The volume of alkaline solution varied for different experiments. Prior to NONOate preparation, 80 ml of phosphate buffer (pH 7.4, 0.1 M) was added to the vessel. The flow loop incorporating the micro-flow cell in the spectrophotometer was also filled with the buffer. Vessel contents were maintained at 37 °C and stirred uniformly at 930 rpm using a caged magnetic stir bar. The headspace was purged for one hour with ultra-pure grade N_2 to remove traces of reactive O_2 or residual NO, if present. The NONOate solution was then injected into the phosphate buffer through the septum port. Spermine NONOate sample (500µl) was injected to obtain a theoretical starting NONOate concentration of 6.9 µM. For Diethylamine NONOate, two different injection volumes were used (see Table III). Injection into the phosphate buffer initiated NONOate decomposition and NO generation. Decomposition of NONOate was spectrophotometrically monitored during the course of the experiment. Absorbances were

TABLE III

PROTOCOL FOR NONOATE SAMPLE PREPARATION

Case	NONOate added to alkaline solution (mg)	Volume of alkaline solution (ml)	Injected volume of NONOate solution* (µl)	Predicted Initial NONOate conc. (µM)
SPERMINE NONOATE				
Runs A-H	10	30	500	6.9
DIETHYLAMINE NONOATE				
Run A Run B-E	10	100	100 200	0.53 1.06

* All NONOate samples injected into 92 ml pH 7.4 (0.1 M) phosphate buffer.

measured every 60 seconds for Spermine NONOate and at 30 second intervals for Diethylamine NONOate. Aqueous NO concentration was simultaneously detected by chemiluminescence.

A sensitivity analysis was carried out to determine the effect of change in temperature on the decomposition rate constant (k_M). The value of k_M was determined at 37 °C and 24 °C, in order to calculate the activation energies for the NONOate decomposition. For determination of k_M at 37 °C, a spectrophotometer with thermostated cell holders was used. NONOate samples were prepared as before in 0.1 M pH 12.0 buffer with 10 mg dissolved in 30 ml for Spermine NONOate and 10 mg in 100 ml for Diethylamine NONOate. Each sample (100 µl) was injected into the pre-warmed pH 7.4 phosphate buffer (0.1 M) in the spectrophotometer cells to achieve starting concentrations of 127 µM and 55 µM, respectively, for Spermine and Diethylamine NONOates. The very slight drop in temperature on injection was taken into account. Absorbance measurements were made at λ =250 nm over time to trace the decomposition of the NONOate. For determination of k_M at room temperature (24 °C), the same procedure was adopted except that the thermostated arrangement was not used.

4.1.2 Minimization of NO reaction.

To minimize the aqueous reaction of NO with residual O_2 from interfering with the analysis, the mass transfer of NO from solution should be much faster than its depletion through reaction. Therefore, to neglect NO reaction in the analysis, it is necessary to minimize

$$\frac{4\,k_1[NO]^2[O_2]}{\left(\frac{k_L A}{V}\right)_{NO}[NO]} \qquad (4.1)$$

The value of k_1 is 2.4×10^6 $M^{-2}s^{-1}$ at 37 °C [Lewis and Deen, 1994]. The NO mass transfer coefficient, $(k_L A/V)_{NO}$, was 0.0048 s^{-1} for all experiments.

Sample preparation methods and injection volumes were designed such that the maximum NO concentration obtained in solution was less than 1 μM. Assuming the system was less than 3 % O_2 saturation (~ 7 μM) for all studies (see section 3.3.2), the maximum ratio of Eq. 4.1 was 0.02 based on a maximum NO concentration of 1 μM. Thus, the reaction of NO with residual O_2 was justifiably neglected for NONOate characterization. However, even at NO concentrations as high as 3 μM, the ratio would only be 0.04.

To check for the minimization of reaction, NO_2^- was measured using the Griess procedure [Dunham, 1995] at the end of each experiment. NO_2^- is a product of the reaction of NO with O_2. Griess solution causes deazotization of NO_2^- to give a pink color proportional to the NO_2^- concentration when measured with a spectrophotometer. A calibration was done with standard NO_2^- solutions prepared in 0.1 M phosphate buffer. Absorbances were measured at λ = 542 nm. The sample and Griess were mixed in a 3: 7 volume ratio. Calibration was linear in the 1-200 μM NO_2^- concentration range (see Figure 6).

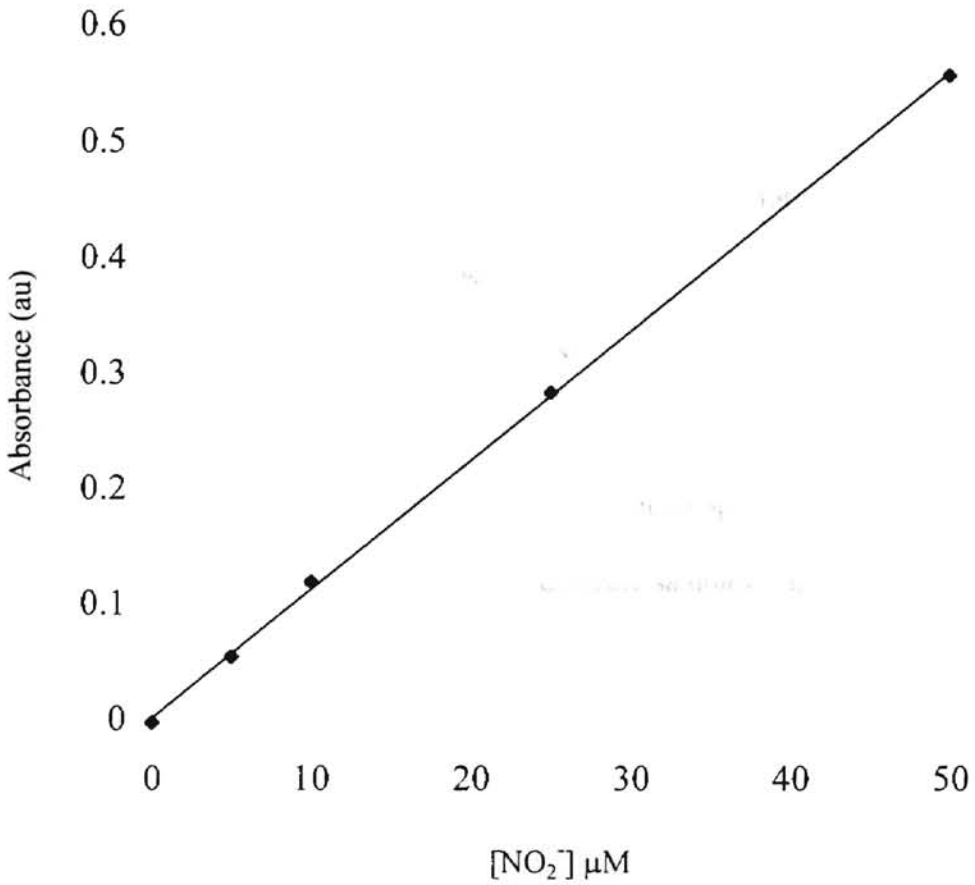

Figure 6. Nitrite calibration using Greiss.

4.1.3 Potential problems.

Experimental parameters such as sample concentration and injection volumes were selected to minimize the reaction of NO with O_2. Preliminary characterization studies involved large initial concentrations of NONOate in the phosphate buffer (~30 μM for Spermine NONOate and ~ 60 μM for Diethylamine NONOate). In addition, the value of $(k_LA/V)_{NO}$ was 0.0023 s^{-1}. With aqueous NO concentrations of up to 6 μM, the ratio of Eq. 4.1 was as high as 0.2. Accordingly, NO reaction in solution, as compared with mass transfer, was substantial. Therefore, the high μM concentrations of NO_2^- formed would have to be taken into account for analysis of NO generated by the NONOates. However, measurements of NO_2^- with time were not feasible since spectrophotometric detection of NO_2^- (at λ=209 nm) was subject to interference by other species such as the NONOates and NaOH (used in preparing the alkaline NONOate sample). Thus, NO reaction with residual O_2 was minimized as described in the previous section.

4.2 Results.

Aqueous NO concentrations were detected by chemiluminescence throughout each experiment as shown in Figures 7 and 8. The NO profiles for Spermine NONOate showed a consistent trend. However, peak NO concentrations varied between 0.51 and 0.72 μM Table IV shows the peak NO concentration obtained for each experiment. For Spermine NONOate experiments, peak aqueous NO concentrations were reached in typically 8-10 minutes and decayed to half its peak value in approximately 55 minutes. Figure 9 shows a typical NONOate decomposition profile for Spermine NONOate using the experimental

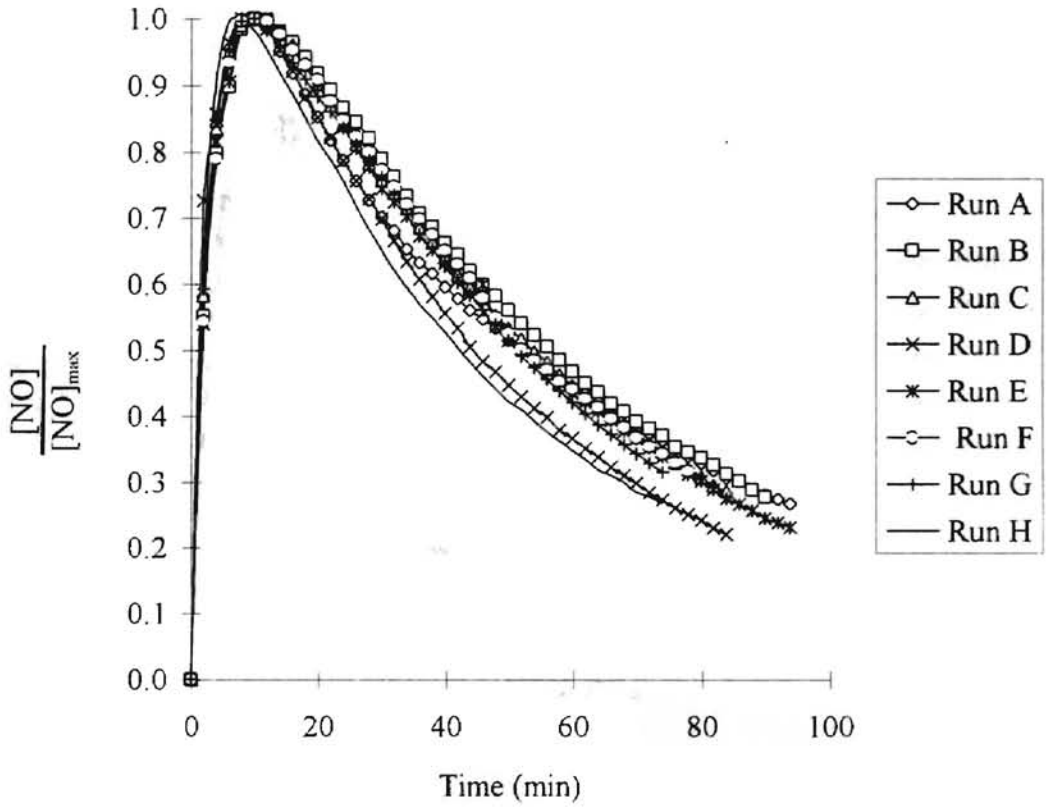

Figure 7. Dimensionless NO profile for Spermine NONOate.
See Tables III and IV for concentration data for individual experiments.

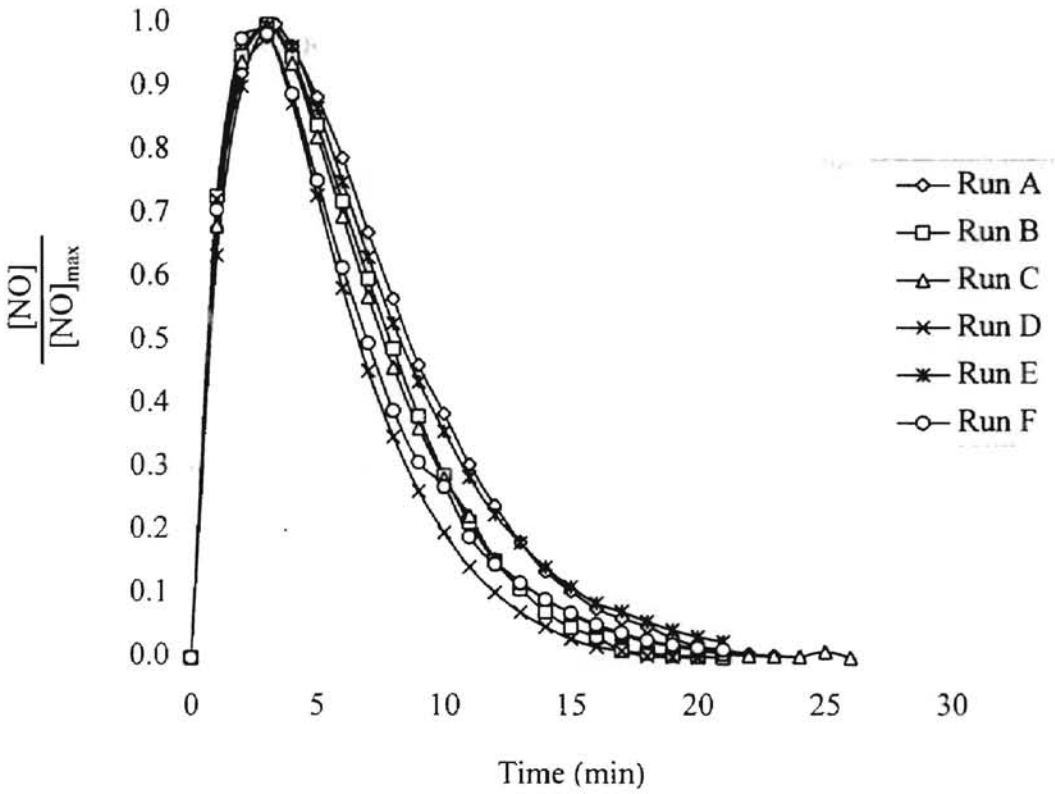

Figure 8. Dimensionless NO profile for Diethylamine NONOate.
See Tables III and IV for individual experiments.

TABLE IV

PEAK AQUEOUS NO CONCENTRATIONS (μM)

Experiment	Spermine NONOate	Diethylamine NONOate
A	0.52	0.48
B	0.52	0.96
C	0.55	1.04
D	0.72	0.81
E	0.51	0.85
F	0.56	
G	0.52	
H	0.51	

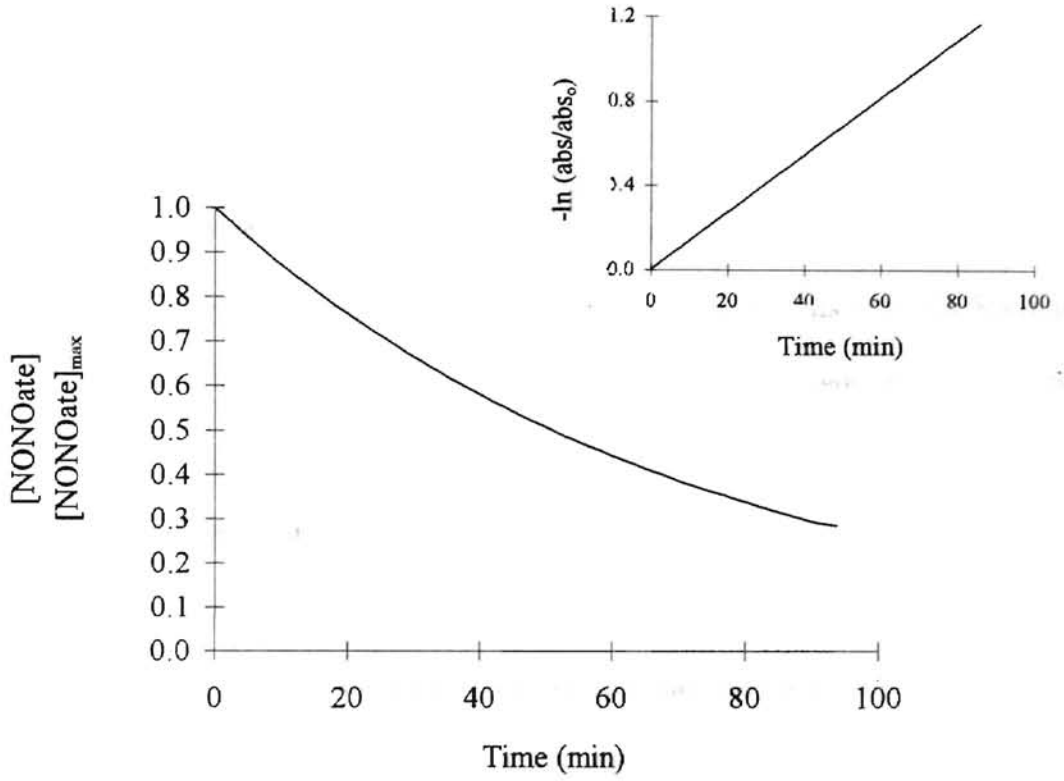

Figure 9. Dimensionless NONOate decomposition profile for Spermine NONOate. Initial NONOate concentration is 6.9 μM at 37 °C. Inset shows the fit to an absorption plot.

setup. The time profile shows exponential decay of the NONOate, as expected with Eq. 2.4. For Diethylamine NONOate, the six runs also showed similar trends, irrespective of the initial NONOate concentration (see Table III). Peak aqueous NO concentrations were obtained within 2 to 3 minutes. The NO profile shows complete depletion of NO from solution within approximately 20 minutes of injection.

4.2.1 Determination of k_M.

The first order rate constant for NO release by the NONOates was determined from the NONOate absorbance data as described in section 2.2.2. Results of k_M for Spermine and Diethylamine NONOates are shown in Table V. The k_M for Diethylamine NONOate decomposition was difficult to determine due to the very low absorbance ranges (< 0.002 absorbance units) encountered within 5-10 minutes of initiating NONOate decomposition. The absorbance appeared to be subject to interference so that accurate estimation of absorbances after the first few minutes was difficult. Thus k_M was obtained using only the first 5 minutes of data. However, preliminary studies with Diethylamine NONOate at much higher starting NONOate concentrations (~60 μM) gave reliable absorbance measurements over the entire experiment resulting in an average k_M of $4.2 \pm 0.6 \times 10^{-3}$ s^{-1}, in close agreement with the value of $3.8 \pm 0.7 \times 10^{-3}$ s^{-1} obtained from initial time data described above. These results are comparable to $5.4 \pm 0.2 \times 10^{-3}$ s^{-1} determined by Maragos et. al (1991). For Spermine NONOate, the average k_M is $0.25 \pm 0.03 \times 10^{-3}$ s^{-1}. This agrees well with $0.30 \pm 0.02 \times 10^{-3}$ s^{-1} determined by Maragos et. al (1991).

TABLE V

k_M FOR SPERMINE AND DIETHYLAMINE NONOATES

Experiment	k_M (10^{-3}) s^{-1}	
	Spermine	Diethylamine
A	0.22	5.0
B	0.25	4.0
C	0.22	2.8
D	0.32	3.7
E	0.25	3.8
F	0.25	
G	0.22	
H	0.24	
Average :	0.25 ± 0.03	3.9 ± 0.8
Preliminary runs:		4.2 ± 0.6

4.2.2 Determination of E_{NO}.

A mass balance of NO in a well stirred aqueous solution is used to determine E_{NO}, as defined in Eq. 2.2, from the NO concentration data. The balance is

$$\frac{d[NO]}{dt} = \text{NO release rate} - 4k_1[NO]^2[O_2] - \left(\frac{k_L A}{V}\right)_{NO}[NO] \qquad (4.2)$$

where the first term is the NO release rate from any NO-releasing compound, the second term is the rate of NO depletion by reaction with O_2, and the third term is the rate of loss of NO from solution by mass transfer. For any NO-releasing compound (M) exhibiting a first order rate of decomposition, such as previously shown for the NONOates (Maragos et al., 1991), the mass balance in a well-stirred system is

$$\frac{-d[M]}{dt} = k_M[M] = \frac{\text{NO release rate}}{E_{NO}} \qquad (4.3)$$

Integration of Eq. 4.3 gives $[M] = [M]_o\, e^{-k_M t}$, where $[M]_o$ is the initial NO-donor concentration. Thus,

$$R_{NO} = k_M[M]_o E_{NO} e^{-k_M t} \qquad (4.4)$$

If E_{NO} is constant, and the reaction term is negligible as justified in section 4.1.2, the rearrangement of Eqs. 4.2 and 4.4 following integration with time gives

$$E_{NO} = \frac{\int_0^t \left(\frac{k_L A}{V}\right)_{NO}[NO]\,dt + [NO]}{[M]_o[1 - e^{-k_M t}]} \qquad (4.5)$$

The numerator indicates the total NO generated in solution up to time *t*. The total NO generated takes into account the net mass transfer of NO from solution, NO by aqueous and the aqueous NO concentration detected by chemiluminescence. The denominator indicates the total number of moles of NO-donor decomposed over the time period considered.

The value of $(k_L A/V)_{NO}$ using the caged stir bar is given in section 3.2.3. For all NONOate characterizations, the initial aqueous NONOate concentration ($[M]_o$) was determined from spectrophotometer absorbance data at the instant the NONOate was added to solution. Reported values of 125 and 154 μM /abs were used for Spermine and Diethylamine NONOate, respectively [Maragos et al., 1991]. For Spermine NONOate, predictions of initial NONOate concentrations (see Table III) and spectrophotometric data agreed closely (< 1-2 % difference). For Diethylamine NONOate, initial NONOate concentrations measured from spectrophotometer data were ~ 30 % greater than predicted. The discrepancy remains unexplained. The initial NONOate concentrations used in Eq. 4.5 for Diethylamine NONOate were those from spectrophotometric absorbance measurements. In determining E_{NO} from Eq. 4.5, the k_M value and NO concentration time profile from each experiment were used. However, for Diethylamine NONOate, the average k_M of preliminary studies (see Table V) was used for all experiments due to the difficulty in measuring k_M at low initial NONOate concentrations.

The E_{NO} profiles obtained for Spermine NONOate are plotted in Figures 10 and 11. The E_{NO} profiles were essentially flat for Spermine NONOate, over a substantial period of the 2 hour experimental duration. As shown in Figure 11, there is a

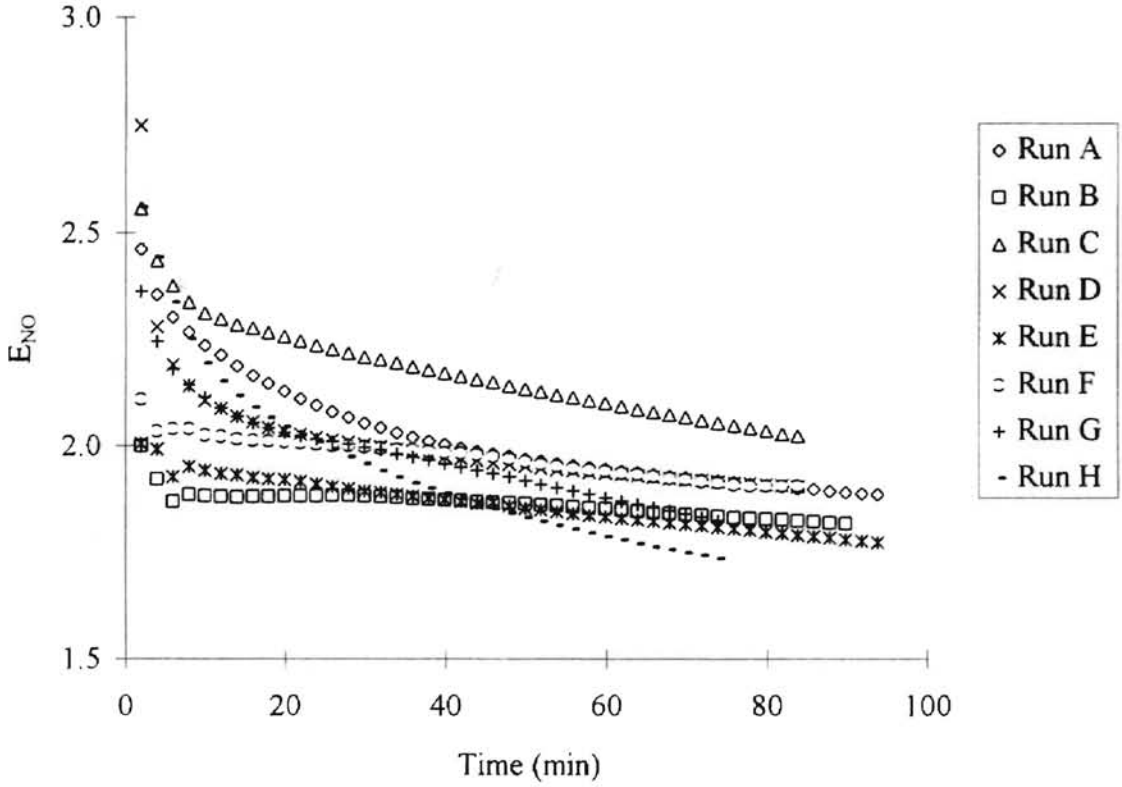

Figure 10. E_{NO} profile for Spermine NONOate.
E_{NO} is defined as the number of moles of NO released per mole of NO-donor decomposed.

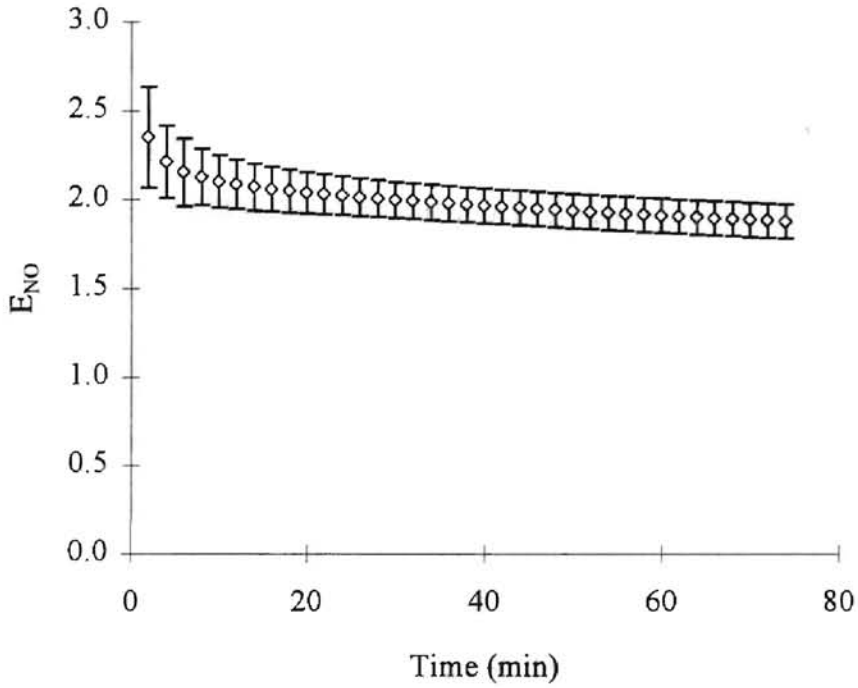

Figure 11. Average E_{NO} profile for Spermine NONOate.
E_{NO} is defined as the number of moles of NO released per mole of the NO-donor decomposed.

slightly higher value for E_{NO} in the first 15 minutes for a k_M value of 0.00025 s^{-1}. Using an activation energy of 1.1 x 10^5 J/mole for the NONOate decomposition, as determined from experiments, k_M values of 0.00028 s^{-1} and 0.00033 s^{-1} respectively, were calculated for one and two degree increase in temperature. Obviously, a slight change in temperature has a significant effect on the value of k_M. The value reported by Maragos et al.(1991) agrees well with the value predicted for a one degree temperature increase above the experimental data reported here. The flow loop in the experimental system was not insulated and there is a possibility that the temperature could slightly decrease. However, the E_{NO} value is still relatively constant over a majority of the time and the E_{NO} value at the end of the experiment is not significantly affected. Using the k_M values for a one and two degree temperature increase with the reported experimental data resulted in E_{NO} values of 1.74 and 1.61, respectively.

The average constant E_{NO} value at pH 7.4 and 37 °C at the end of the experiment was 1.87 ± 0.08 and 1.69 ± 0.07 for k_M values of 25 x 10^{-5} s^{-1} and 30 x 10^{-5} s^{-1}, respectively. Comparing this with the E_{NO} value of 1.90 determined for Spermine NONOate at pH 2.0 [Maragos et al., 1991], it is apparent that the E_{NO} is slightly sensitive to the pH, at worst. Decomposition of Spermine NONOate was not complete at the end of the experiment although the E_{NO} value approached a constant value within 20 minutes. Table VI gives the E_{NO} values obtained at the end of each Spermine NONOate experiment. Figures 12 and 13 show the E_{NO} for Diethylamine NONOate. The profiles show an initial E_{NO} value greater than the theoretical limit of 2. The average E_{NO} at the end

TABLE VI

E_{NO} FOR SPERMINE AND DIETHYLAMINE NONOATES

Experiment	E_{NO}	
	Spermine	Diethylamine
A	1.89	1.59
B	1.82	1.70
C	2.02	1.53
D	1.90	1.34
E	1.81	1.35
F	1.91	
G	1.82	
H	1.74	
Average :	1.87 ± 0.08	1.50 ± 0.16

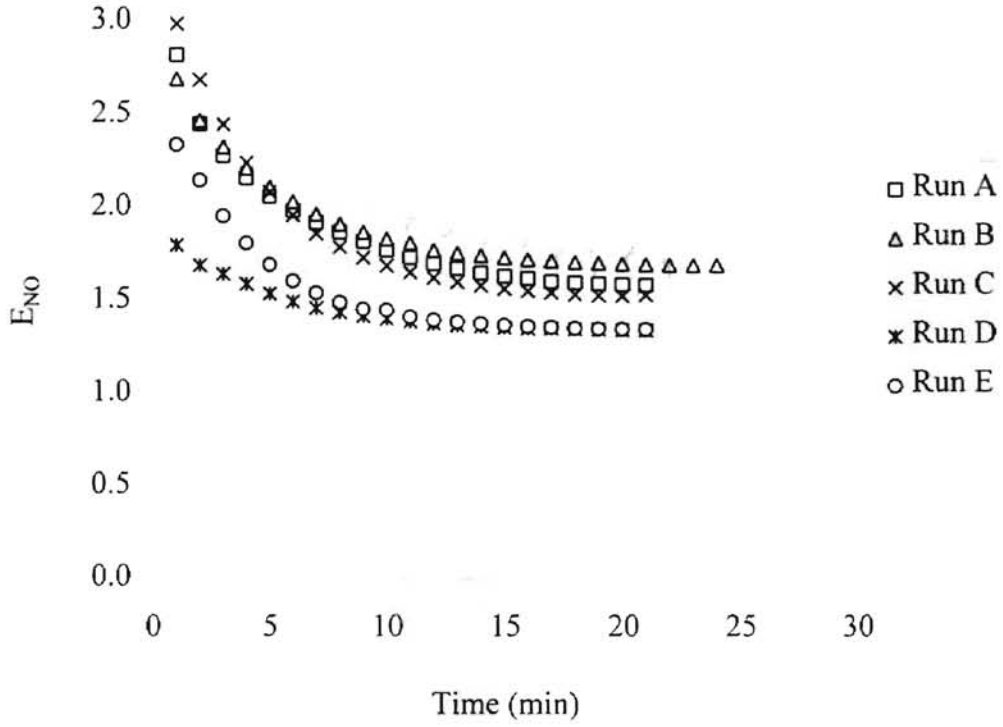

Figure 12. E_{NO} profile for Diethylamine NONOate.
E_{NO} is the number of moles of NO released per mole of NO-donor decomposed.

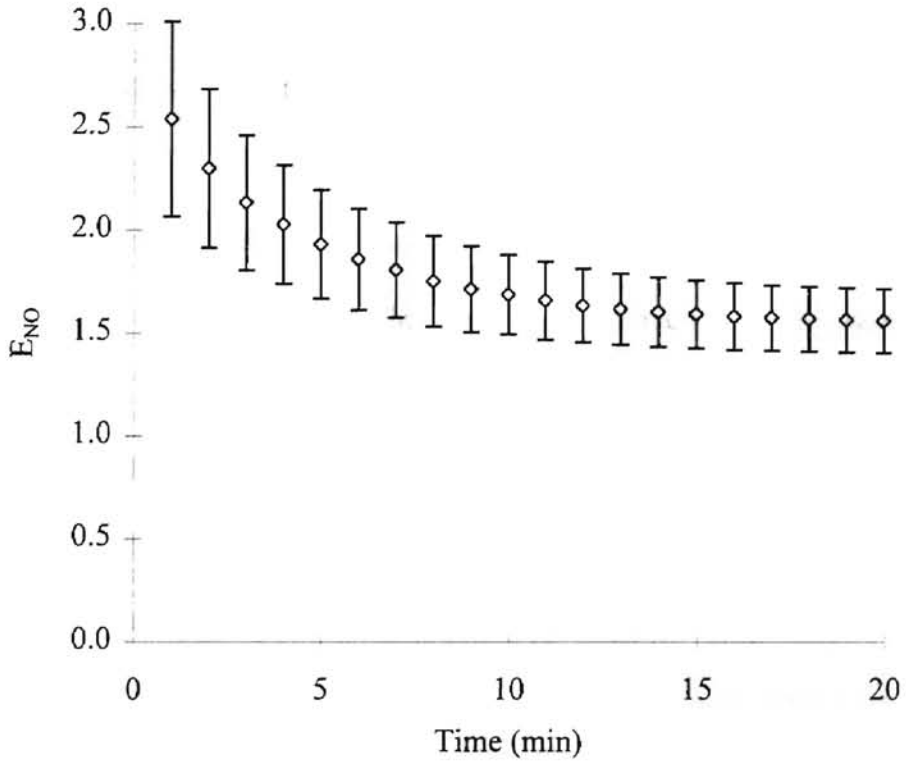

Figure 13. Average E_{NO} profile for Diethylamine NONOate. E_{NO} is the number of moles of NO released per mole of NO-donor decomposed.

of the experiment for Diethylamine NONOate was 1.50 ± 0.16 (see Table VI). This compares favorably with the 1.50 ± 0.11 obtained by Maragos et al. (1991).

As in the case of Spermine NONOate, an activation energy of 1.0×10^5 J/mole was experimentally determined for Diethylamine NONOate decomposition. From this, k_M values of 0.0048 s^{-1} and 0.0053 s^{-1}, respectively, were determined for a one and two degree temperature increase. The k_M value reported by Maragos et al. corresponds to the k_M estimated for a two degree temperature increase over the experimental data reported here. The initial part of theE_{NO} profile flattens out when successively higher k_M values are used for its determination. For the Diethylamine NONOate study, complete NONOate decomposition was achieved at the end of the experiment. Thus, k_M was not necessary for determining the E_{NO} value at the end of the experiment.

NO_2^- analysis was carried out at the end of each experiment to confirm the minimization of the reaction of NO with O_2. In most of the experiments, the aqueous NO_2^- concentrations were less than 1 μM indicating negligible reaction of NO. However, the analysis was not completely reliable for Spermine NONOate owing to the fact that NONOate decomposition and thus NO formation were continued and not completed prior to analysis. Thus, NO generated during the analysis could lead to significant NO_2^- formation since the samples were exposed to air.

4.3 Conclusions.

Successful characterization of Spermine and Diethylamine NONOate was carried out. The E_{NO} values at the end of each experiment for both Spermine and Diethylamine NONOates agreed well with literature. The highlights of the modified characterization protocol adopted in this study were :

a) Aqueous NO concentrations were directly measured via chemiluminescence, which facilitated shorter experimental duration (~ 2 hours for Spermine NONOate) and enabled E_{NO} to be determined even before complete decomposition of the NONOate. This is valuable for assessing E_{NO} at pH values in which decomposition is slow.

b) Depletion of aqueous NO through mass transfer was accounted for by determination of the volumetric mass transfer coefficient for NO. Loss of NO by aqueous reaction with O_2 was rendered insignificant by maintaining reaction free conditions. This ensured a more accurate analysis of the NO generated by the NONOates.

c) A direct consequence of (a) was that Spermine NONOate could be characterized at physiological pH.

d) E_{NO} was determined as a function of time. The E_{NO} versus time profile showed that E_{NO} was essentially constant for Spermine NONOate.

e) E_{NO} at the end of each experiment and k_M values obtained for both Spermine NONOate and Diethylamine NONOate agreed well with literature. However, Spermine NONOate was not previously characterized for E_{NO} at pH 7.4.

The major impact using the method previously described is that it is generally applicable not only to NONOates, but to all NO-donor compounds. Eq. 4.2 can be used to determine the NO-release rate from NO concentration versus time data when reaction is minimized or absent. If a model for NO-release is available, the model parameters can be determined from the NO-release rate data. This in turn can be used to predict the NO concentration versus time data for the experimental system, even in the presence of reactions.

CHAPTER 5

MODELING OF NO RELEASE IN AQUEOUS SOLUTIONS

The purpose of characterizing NONOate compounds was to determine the kinetic parameters of NO release, specifically, E_{NO} and k_M. Knowledge of the kinetics of NO release in aqueous solution provides a basis for the development of models to predict NO concentrations generated in solution following dissolution of a NONOate compound. In the first experiments (Chapter 4), E_{NO} and k_M were determined in O_2-free systems with the intent of minimizing reaction of NO in solution. However, the model developed in this chapter pertains to NO concentration predictions in oxygenated aqueous media.

The validity of the model is explored with three different oxygenated media : (a) phosphate buffer, (b) culture media and (c) Tyrode's albumin buffer. Validation of the model in such media would be useful for making theoretical estimations of the NO concentration levels achievable on dissolution of known amount of NONOates. Thus, the model would be convenient for experimentally assessing the effects of NO concentration in biological systems. The E_{NO} profiles obtained for Spermine NONOate (Chapter 4) show that E_{NO} is essentially constant throughout the duration of the experiment. For validation of the model developed in this chapter, Spermine NONOate was used.

5.1 Experimental materials and methods.

A major difference between the NONOate characterization protocol and the protocol explained below is that the latter involves oxygenated solutions. Under these conditions,

aqueous reaction of NO with O_2 in solution is important for NO analysis. Oxygenated solutions are used to represent biological systems where oxygen is present. It is for the same reason that the validity of the model is tested in aqueous solutions containing culture medium with serum since this solution contains components found *in vivo*. The preparation methods and experimental protocol for phosphate buffer, culture media and Tyrode's solution are discussed in the following sections.

5.1.1 Phosphate buffer.

Phosphate buffer (0.1 M, pH 7.4, 80 ml) was added to the modified ultrafiltration cell. In addition, the flow loop was filled with 12 ml of the buffer. The buffer was pumped through the flow loop during the experiment at a flow rate of 70 cc/min. A caged stir bar was used to rapidly stir the vessel contents. Air was passed through the head space to saturate the buffer with oxygen.

5.1.2 Culture media.

Reagents- Dubecco's modified Eagle's medium (D-MEM) without phenol red, sodium pyruvate or sodium bicarbonate was purchased from Life Technologies, Inc.(Grand Island, NY). Donor calf serum and HEPES buffer were also obtained from Life Technologies Inc Sodium pyruvate was purchased from Sigma. Sodium bicarbonate was purchased from EM Science Inc. (Gibbstown, NJ).

Preparation- D-MEM, 3.7 g sodium bicarbonate, 10 ml sodium pyruvate, 20 ml HEPES buffer, and 100 ml donor calf serum were added to deionized water to make up

1000 ml of solution. The pH was adjusted to 7.4 by dropwise addition of 0.01 M HCl or 0.01 M NaOH.

Method- Buffer capacity was maintained by passing a 5 % CO_2, balance air mixture through the head space. Owing to the denaturing of the proteins in solution when pumped using a gear pump, flow through the flow loop was avoided. Therefore, 92 ml of the culture medium was accordingly added to the vessel. To prevent frothing and denaturing of the media components, slow speed stirring (85 rpm) was carried out using a polysulfone stirrer. Initial warming of the culture media was done in a water bath half hour prior to starting each experiment. Initial warming in the oven was avoided because of overheating and subsequent denaturing of the solution. Overheating would cause the clear solution to turn cloudy.

5.1.3 Tyrode's solution.

Tyrode's solution is a buffer used in biological applications. As with culture media, easily denatured protein components (albumin) makes it imperative for preparation and storage of the buffer under carefully maintained conditions.

Reagents- $NaHCO_3$, KCl, and Na_2HPO_4 were purchased from EM Science, Inc.(Gibbstown, NJ). NaCl, $MgCl_2$ and $CaCl_2$ were obtained from Fisher Chemicals (Fairlawn, NJ). HEPES buffer was obtained from Life Technologies Inc. Glucose and bovine albumin (Ca^{2+} and fatty acid free) were obtained from Sigma (St. Louis, MO).

Preparation- 154 mM NaCl, 2.7 mM KCl, 12 mM $NaHCO_3$, 0.35 mM Na_2HPO_4, 1.2 mM $MgCl_2$, 2 mM $CaCl_2$, 5.5 mM glucose and 0.35 % bovine albumin were added to

deionized water to make 1000 ml of the buffer. The pH was adjusted to 7.35 and stabilized with 2.5 mM HEPES.

Method - As with the culture media studies, 92 ml of the buffer was added and the flow loop was not used. To avoid frothing, slow stirring of the buffer was carried out using a polysulfone stirrer. The head space was purged with 5 % CO_2, balance air mixture. The CO_2 was added to maintain the buffer capacity. Unused solution was stored at 0 °C to prevent denaturing. The buffer was heated to 37 °C in a water bath prior to its use.

5.1.4 General protocol.

Aqueous solution (80 or 92 ml) was added to the vessel depending on if the liquid was pumped through the flow loop or not. The liquid was maintained at 37 °C in an oven. Uniform stirring was maintained. An air or CO_2-air mixture was passed through the headspace for 1 hour prior to NONOate injection so as to achieve near O_2-saturation of the buffer. The air/CO_2-air mixture flow through the head space was continued over the entire period of the experiment. In all cases preliminary studies showed that 87 % saturation of O_2 was obtained. Aqueous NO concentrations obtained subsequent to Spermine NONOate introduction were detected by chemiluminescence.

All NONOate samples were prepared as in the method described in section 4.1.1. In order to avoid any pH increase due to injection of a strongly alkaline solution, alkaline buffer (0.01 M NaOH + 0.01 M Na_2HPO_4) of pH 12 was used instead of the 0.1 M alkaline buffer utilized in NONOate sample preparation for characterization studies. Validation of the model in phosphate buffer was carried out at three different initial

NONOate concentrations (Table VII). This allowed for checking the validity of the developed model at different NO concentration ranges and for investigating possible concentration-dependent effects occurring in solution. Table VII summarizes the details for Spermine NONOate sample preparation, injection volumes, and initial NONOate concentrations. All experiments carried out in culture media and Tyrode's albumin buffer involved injection of high NONOate concentrations only (Case A). Following each experiment, the pH was measured.

5.2 Model Development.

The objective of developing a model is to enable predictions of aqueous NO concentrations obtained on dissolution of theoretical amounts of NONOates in an oxygenated solution. For a well stirred system containing NONOate, the mass balance of NO is represented by Eqs. 4.2 and 4.4 as

$$\frac{d[NO]}{dt} = [M]_o k_M E_{NO} e^{-k_M t} - \left(\frac{k_L A}{V}\right)_{NO} [NO] - 4k_1[NO]^2[O_2] \qquad (5.1)$$

$[M]_o$ is obtained theoretically and not from NONOate absorbance measurements as done previously during characterization. Table VII gives the $[M]_o$ values for different cases. The first order rate constant k_M is 0.00025 s^{-1} as determined by NONOate characterization (see section 4.2.1). An E_{NO} value of 1.87 for Spermine NONOate is used since E_{NO} for Spermine NONOate is essentially constant.

TABLE VII

PROTOCOL FOR NONOATE SAMPLE PREPARATION

Case	NONOate added to alkaline solution (mg)	Volume of alkaline solution (ml)	Injected volume of NONOate solution (μl)	Predicted initial NONOate conc. (μM)
Case A	10	1	200	82.7
Case B	10	30	500	6.9
Case C	10	30	250	3.45

The second term in Eq. 5.1 represents the rate of depletion of aqueous NO due to mass transfer across the gas-liquid membrane and through the composite membrane at the bottom of the vessel. Rapid stirring used for experiments in phosphate buffer resulted in a value of 0.0048 s^{-1} for $(k_LA/V)_{NO}$. Experiments involving culture media or Tyrode's buffer used slow stir speeds. For application of the model to such cases, a volumetric mass transfer coefficient of 0.00168 s^{-1} is used as shown in Table II of Chapter 3.

The third term is the rate of consumption of aqueous NO by reaction with O_2. The reaction rate constant, k_1, is 2.4 x 10^6 M^{-2} s^{-1} [Lewis and Deen, 1994]. The squared dependence of this term on the NO concentration shows that an non-linear increase occurs in the reaction rate with increasing NO concentration. For NO predictions in the absence of reaction, this reaction is altogether neglected. An O_2 concentration of 87 % saturation was used in the model, based on the concentrations observed during preliminary studies. The saturated aqueous O_2 concentrations are 230 μM when air is used to oxygenate the solution and 219 μM when a 5 % CO_2, balance air mixture is used. High levels of O_2 in the system ensure insignificant depletion of O_2 due to reaction. Therefore, change in the O_2 concentration does not have to be taken into account for solving Eq. 5.1. The NO balance is solved analytically using the Mathcad mathematical package. Appendix A lists the format of a sample calculation procedure.

5.3 Results.

The model was used to check the validity of predictions of aqueous NO concentrations with experimental results.

5.3.1 Model validation with phosphate buffer.

The model validity was evaluated at three different starting NONOate concentrations with phosphate buffer. For case A, with a theoretical initial NONOate concentration of 82.7 μM, four experiments were performed. Experimental and predicted NO profiles are shown in Figures 14 and 15. NO profiles obtained in runs 1, 2 and 4 agreed closely with the NO profile generated by the model in the presence of aqueous NO reaction. The average peak concentration obtained experimentally (3.54 ± 0.75 μM) compared well with that predicted by the model with reaction (3.15 μM) as shown in Figure 15. In comparison, the peak NO concentration generated by the model in the absence of reaction was 6.84 μM. Thus, the importance of including the reaction term can be seen. The large error margin was due to a single outlying profile (Run 2). The time in which the maximum NO concentration was achieved agreed well between experiments and the model. As the depletion of NO occurs, the importance of the reaction term in Eq. 5.1 is diminished.

Case B involved a theoretical starting NONOate concentration of 6.9 μM. NO profiles obtained in runs 1-6 are compared with model generated profiles in Figure 16. Profiles from experiments 1, 3 and 6 agreed closely with the NO profile predicted by the model which included aqueous reaction. Experiments 2, 4 and 5 displayed higher levels of NO depletion but their profiles were in general agreement. The peak average concentration

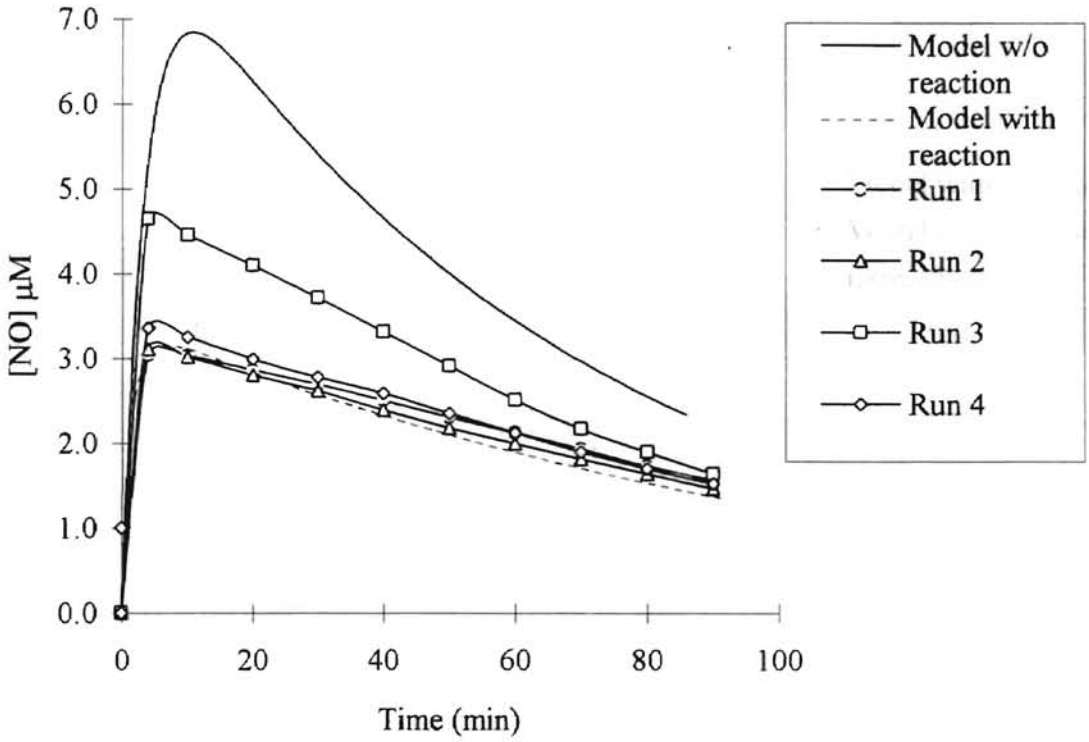

Figure 14. Model and experimental NO profiles with phosphate buffer : Case A for 4 runs. (see Table VII)

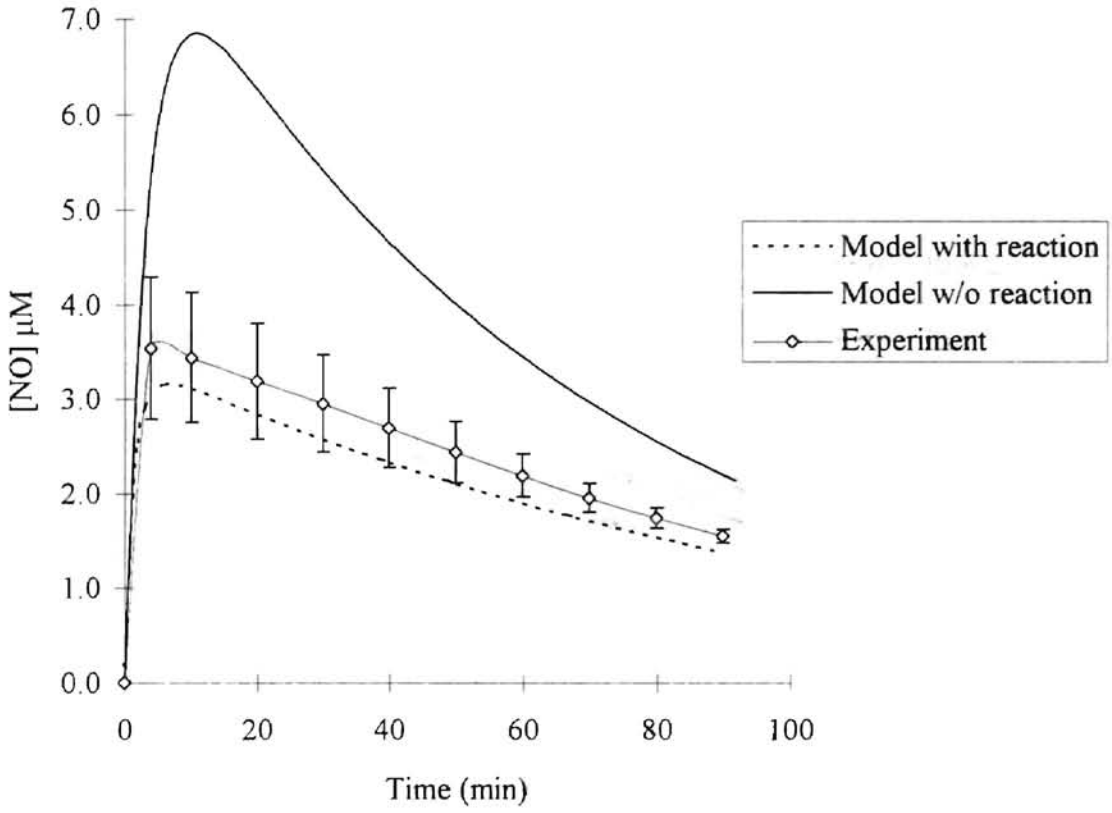

Figure 15 Average NO profile with phosphate buffer: Case A. (see Table VIII).

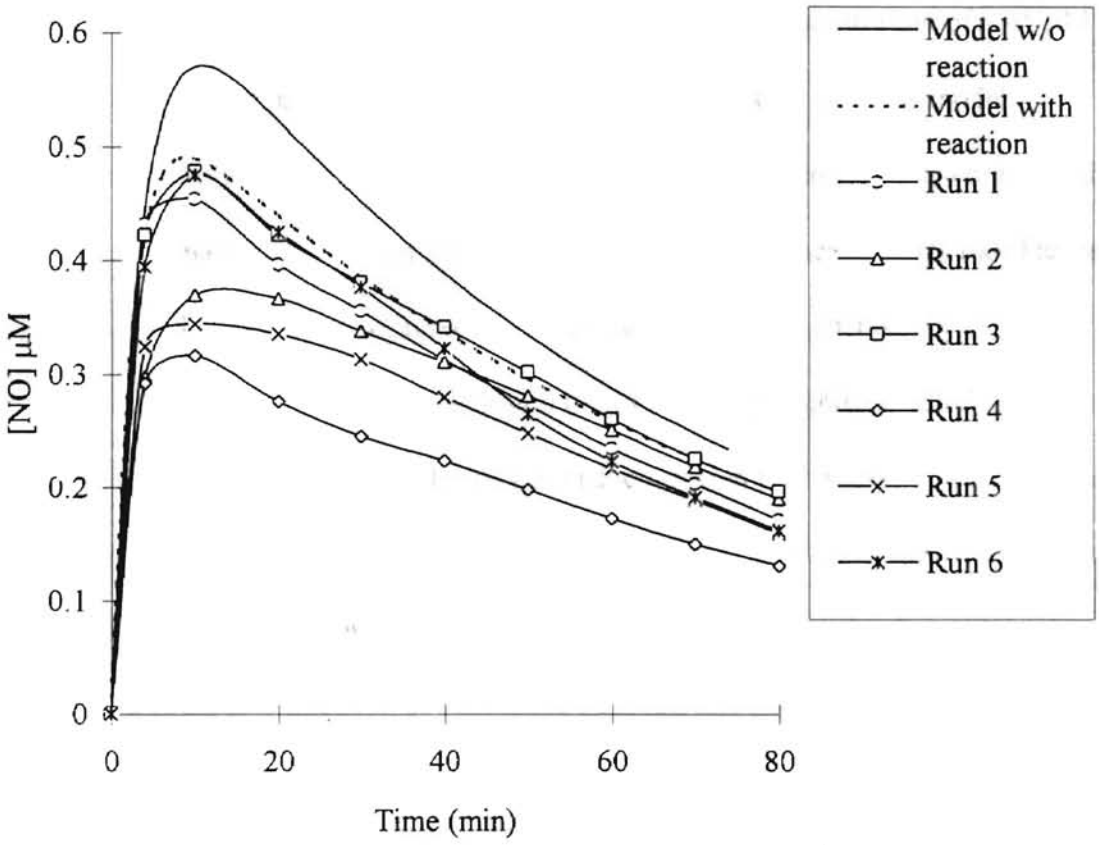

Figure 16. Model and experimental NO profiles with phosphate buffer : Case B for 6 runs.(see Table VII).

obtained from all experiments (0.41 ± 0.07 μM) generally agreed with that predicted by the model (0.49 μM). In addition, the peak NO concentration was attained at similar times for the experiments and the model as shown in Figure 17. In comparison, when reaction was neglected in the model, the peak NO concentration predicted was slightly higher at 0.57 μM.

Case C involved a theoretical starting aqueous NONOate concentration of 3.45 μM. Trends in the experimental NO profiles were generally consistent with the model predictions as shown in Figure 18. Errors in injection of NONOate possibly contributed to the large error margin observed at such low initial NONOate concentrations (see Figure 19). Runs 5 and 6 showed close agreement with the NO profile generated by the model which included reaction. However, exclusion of reaction only slightly affected the model predictions since the reaction term becomes small compared to the mass transfer term at low NO concentrations. The peak NO concentration obtained in run 2 was much higher than predicted even in the absence of reaction. This suggested that the discrepancy was possibly due to error in injection of NONOate samples, and not due to the absence of reaction. This may have been the case with runs 3 and 4 which produced lower aqueous NO concentration levels.

Table VIII shows the peak NO concentrations predicted by the model in phosphate buffer as compared with the experimental NO concentrations. Use of constant parameters in the model was justified by the observation that pH of the solution remained unchanged for all experiments.

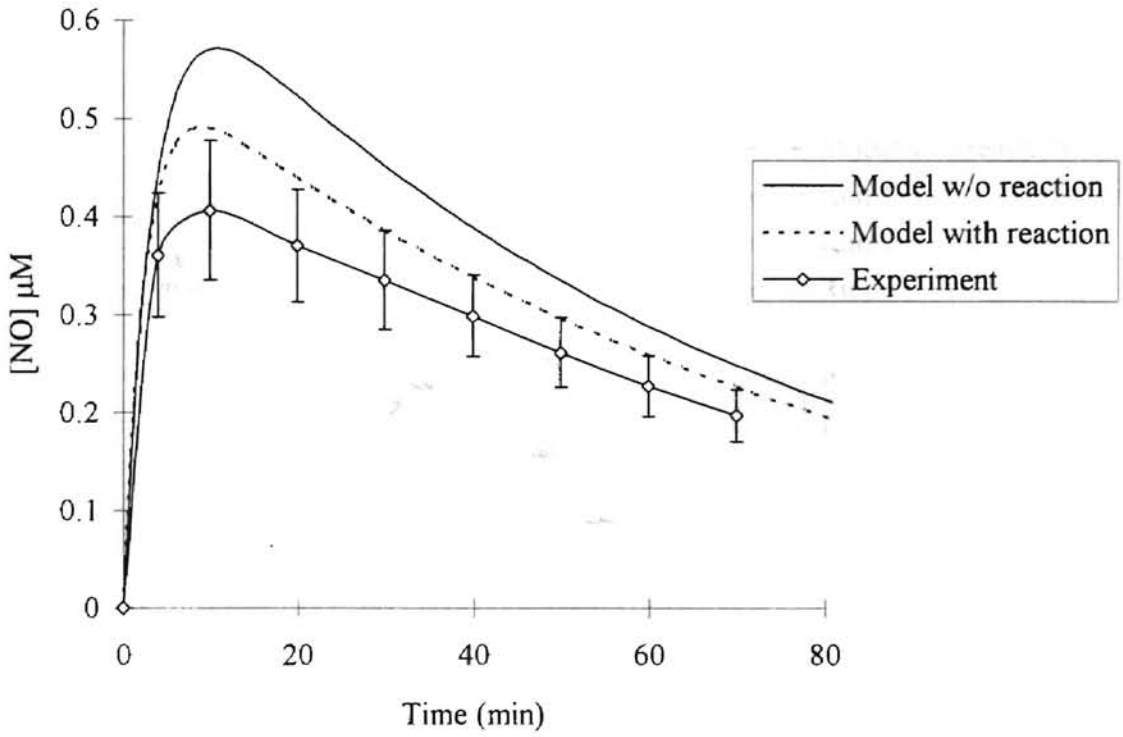

Figure 17. Average NO profile with phosphate buffer . Case B. (see Table VIII).

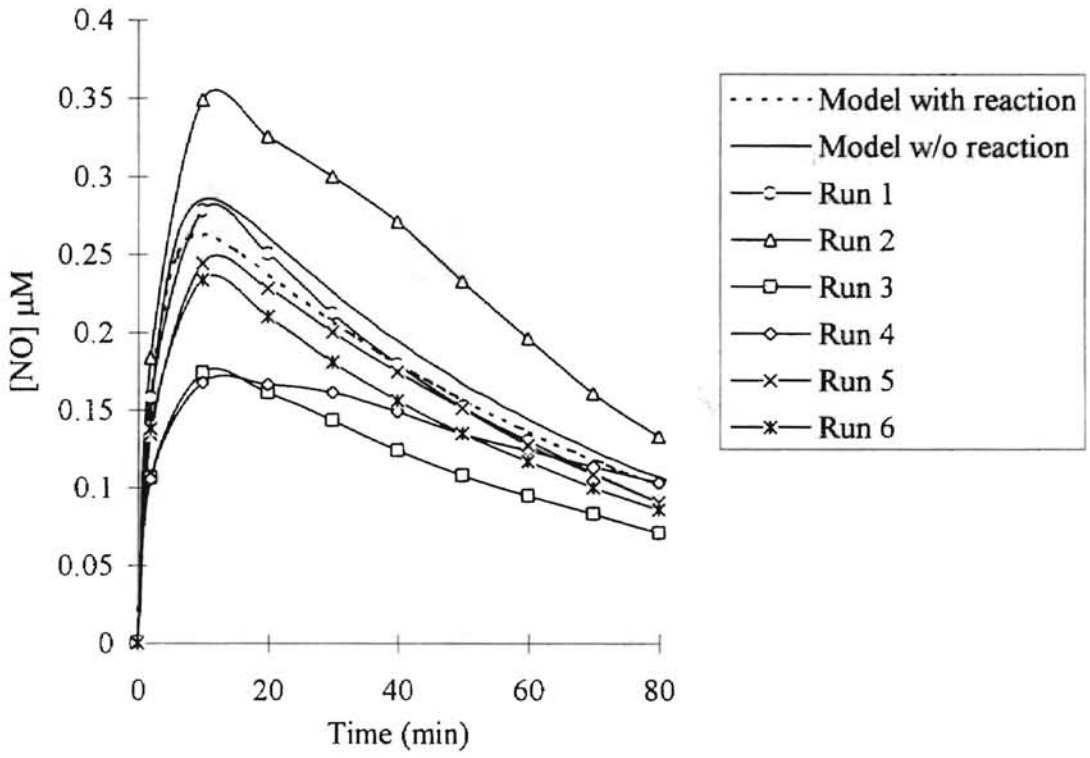

Figure 18. Model and experimental NO profiles with phosphate buffer : Case C for 6 runs. (see Table VII).

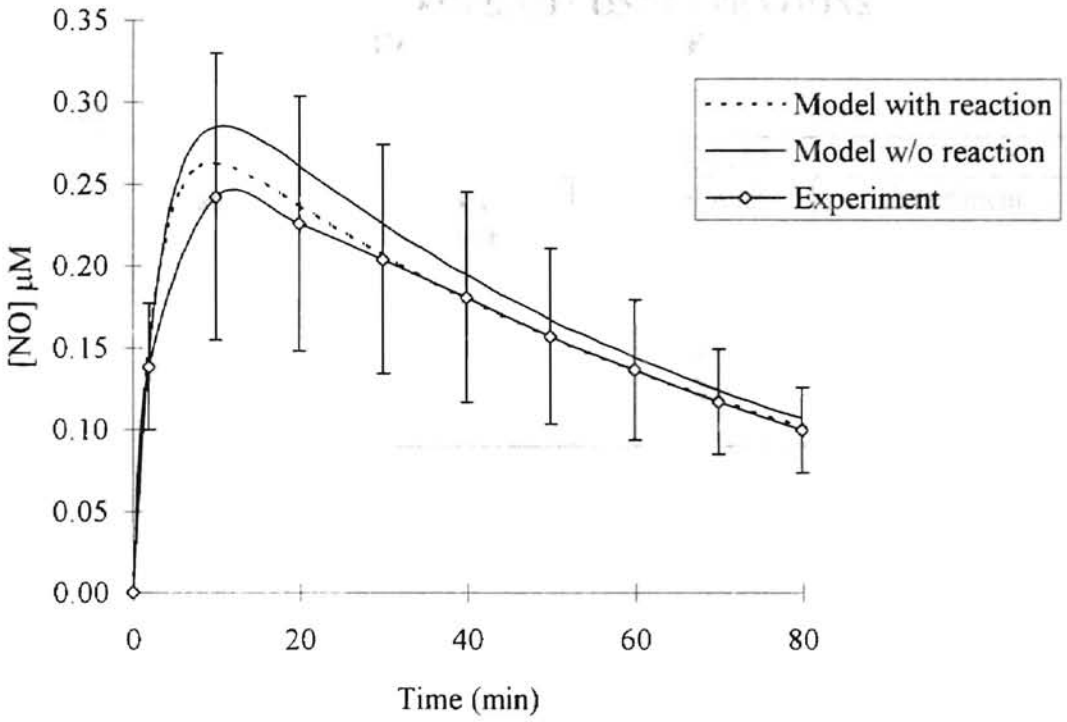

Figure 19. Average NO profile with phosphate buffer : Case C. (see Table VIII).

TABLE VIII

PEAK AQUEOUS NO CONCENTRATIONS IN PHOSPHATE BUFFER

Case	[NO] uM		
	Model without reaction	Model with reaction	Experiment
A	6.84	3.15	3.54 ± 0.75
B	0.57	0.49	0.41 ± 0.07
C	0.29	0.26	0.24 ± 0.09

5.3.2 Model validation with culture media.

A theoretical starting NONOate concentration of 82.7 μM was used for all experiments with culture media. As shown in Figure 20, very good agreement was observed between the experimental NO profiles and those predicted by the model which included reaction of NO. The peak NO concentrations obtained from the model with and without reaction were 16.49 μM and 3.90 μM, respectively. The peak average NO concentration obtained from experiment was 3.57 $\pm$ 0.27 μM, in good agreement with the model. The average experimental NO profile is shown in Figure 21. The error margin in the experimental NO concentrations was at most 8.5 %. Peak NO concentrations were obtained in ~ 6 minutes when reaction was considered (both experimental and model) and ~ 22 minutes for the NO profile generated by the model in absence of reaction. In all cases, the pH of the solution remained unchanged.

5.3.3 Model validation with Tyrode's buffer.

A theoretical initial NONOate concentration of 82.7 μM was used in all studies with Tyrode's buffer. The peak NO concentrations predicted by the model with and without reaction were 3.90 and 16.49 μM, respectively. As shown in Figure 22, experimental NO profiles agreed well with model predictions in the presence of reaction. Figure 23 shows the average experimental NO profile. The peak average NO concentration obtained experimentally was 3.77 $\pm$ 0.37 μM, in good agreement with the model.

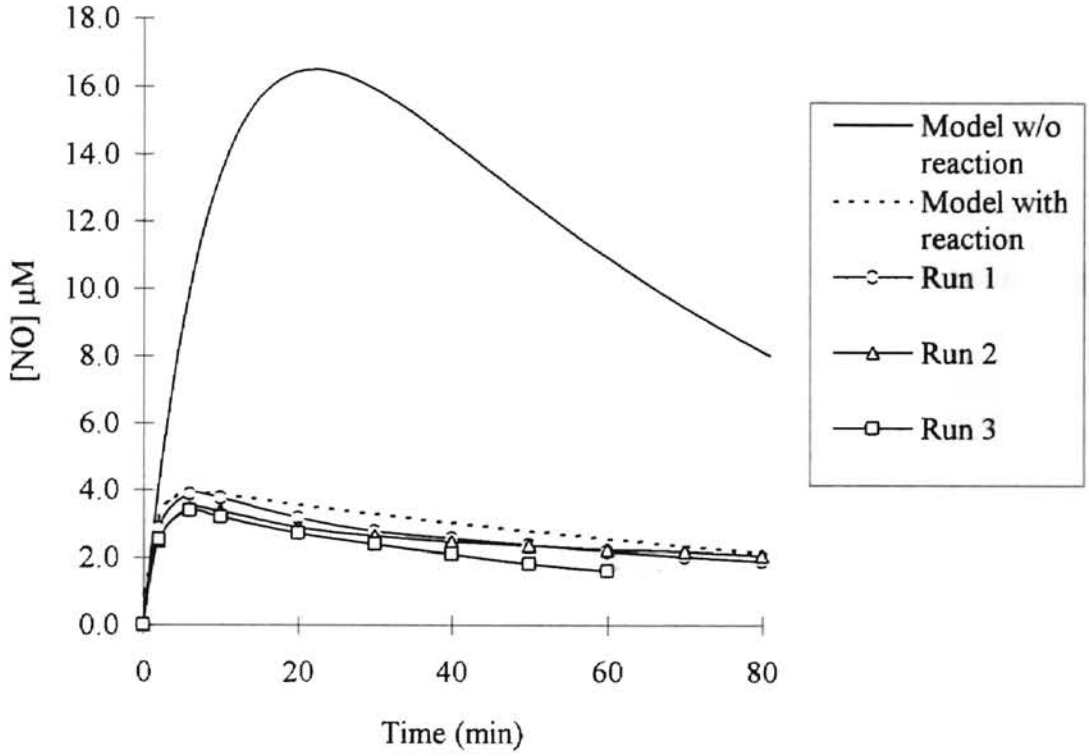

Figure 20. Model and experimental NO profiles in culture media. (see Case A in Table VII).

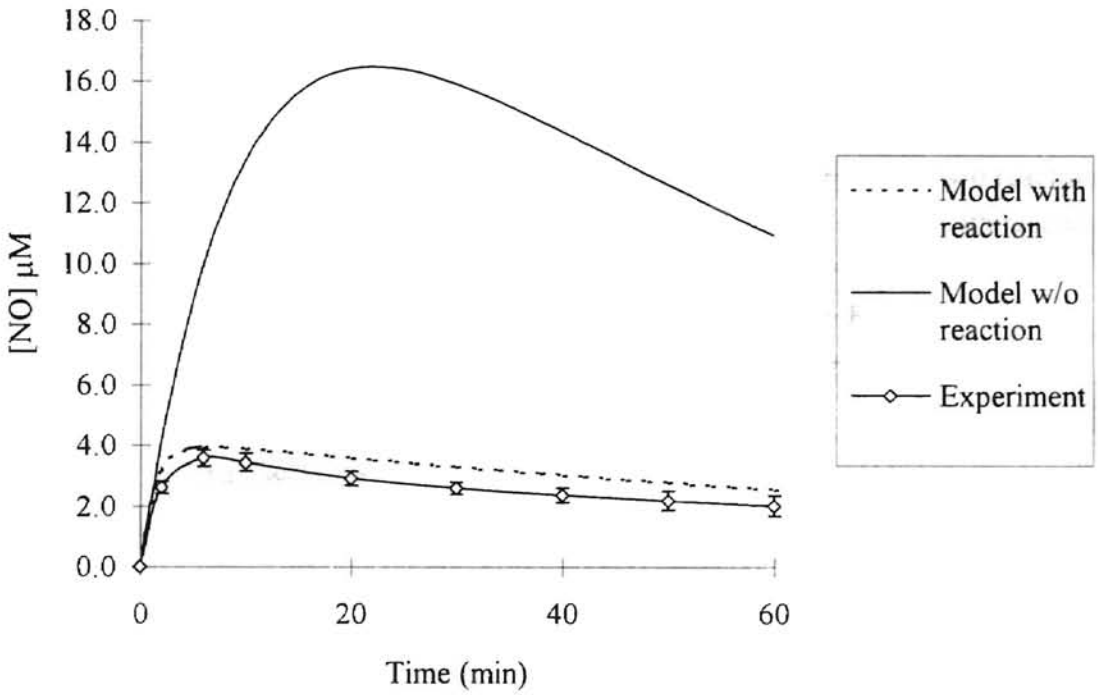

Figure 21. Average NO profile with culture media.

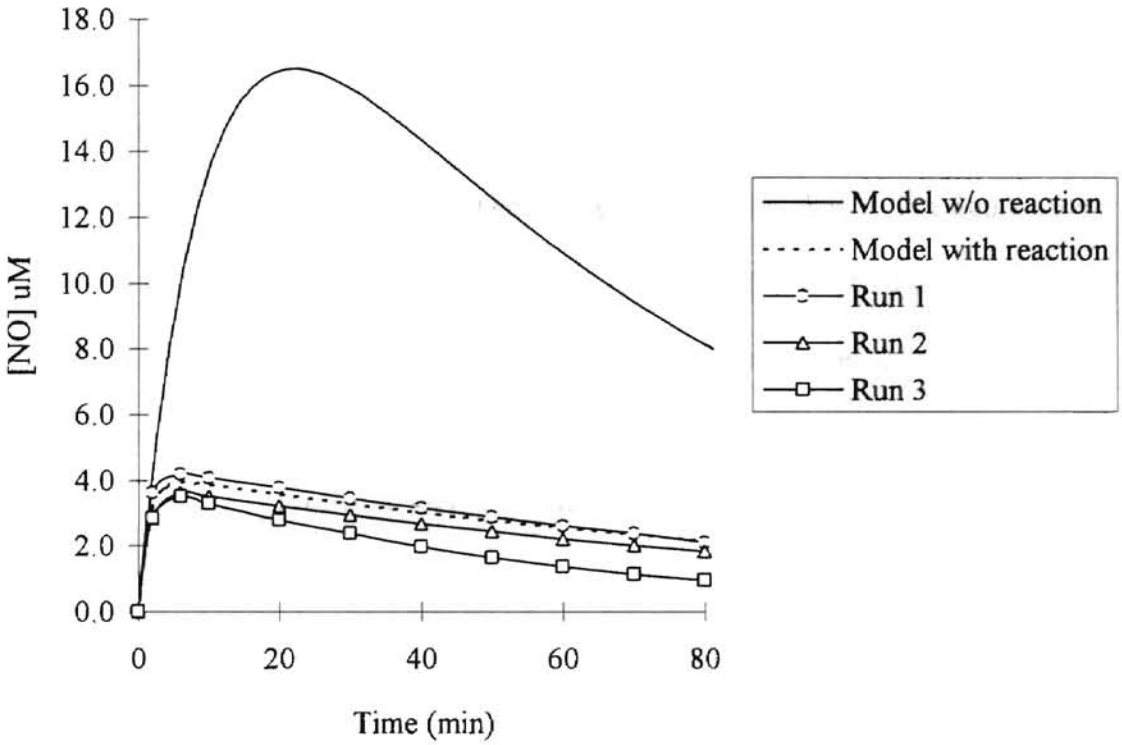

Figure 22. Model and experimental NO profiles with Tyrode's solution. (see Case A in Table VII).

5.3.4 Effect of k_M on model predictions.

The average value of 0.00025 s^{-1} for k_M and an E_{NO} of 1.87, determined from the NO concentration versus time data using this rate constant, was used in the model. It was observed that using higher k_M value yielded a lower constant E_{NO} value. The sensitivity of the model to the k_M value and the derived E_{NO} value was checked by generating NO profiles using different values for these parameters in the model. Figure 24 shows the effect of k_M on NO concentration predictions with Tyrode's buffer. The average NO profile obtained from experiment with Tyrode's solution is also shown. The figure shows that as the k_M incorporated in the model is increased from 2.5×10^{-5} to 3×10^{-5} s^{-1} (the literature value), the peak height of the generated NO profile is increased from 3.90 to 4.02 μM. It is apparent from the figure that with a faster k_M, the decay of the NO profile occurs more rapidly and the peak NO concentration is higher. It was observed that whatever k_M and E_{NO} values were used in the model, the product of the two terms is not very different. The NO-release term in the model, is therefore not significantly affected. As a result, the NO-release predictions determined from different sets of parameters are similar. As the characterization studies showed slightly different k_M values for each run, minor deviations of model predictions from experimental data can possibly be due to slight differences between the average k_M value used in the model and the actual k_M value of each experiment. As mentioned earlier in section 4.2.2, minor deviation of the average k_M obtained from the actual k_M value, could have been due to a slight drop in temperature over the flow loop.

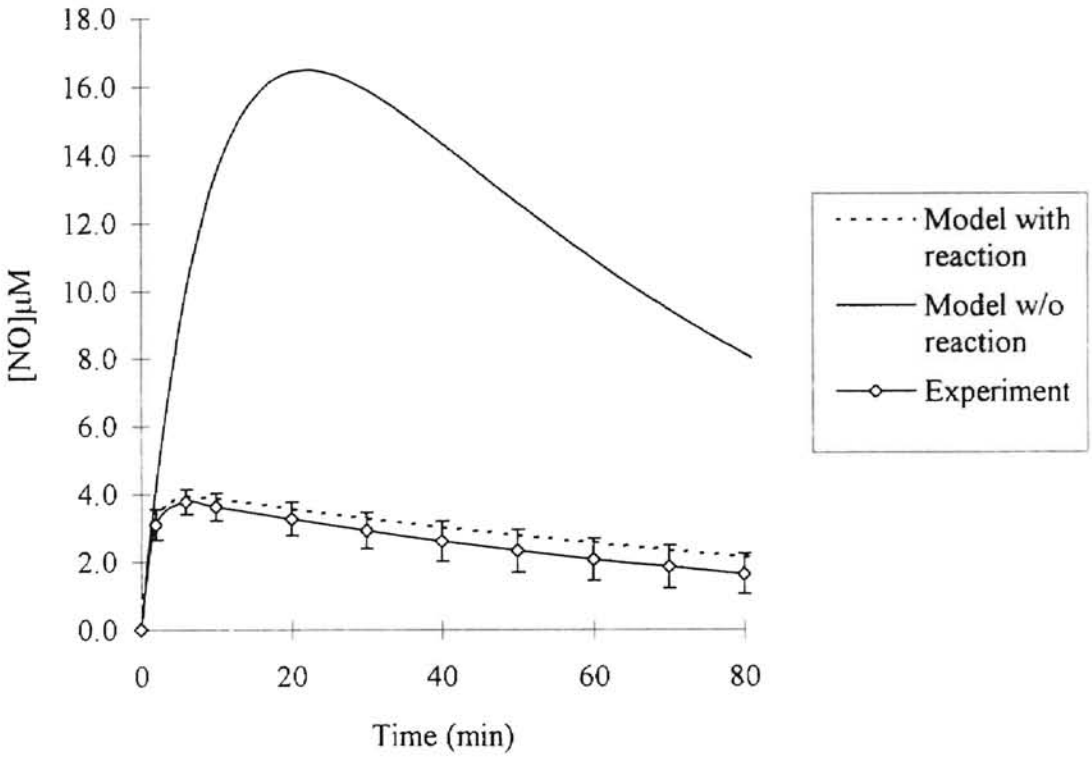

Figure 23. Average NO profile with Tyrode's solution.

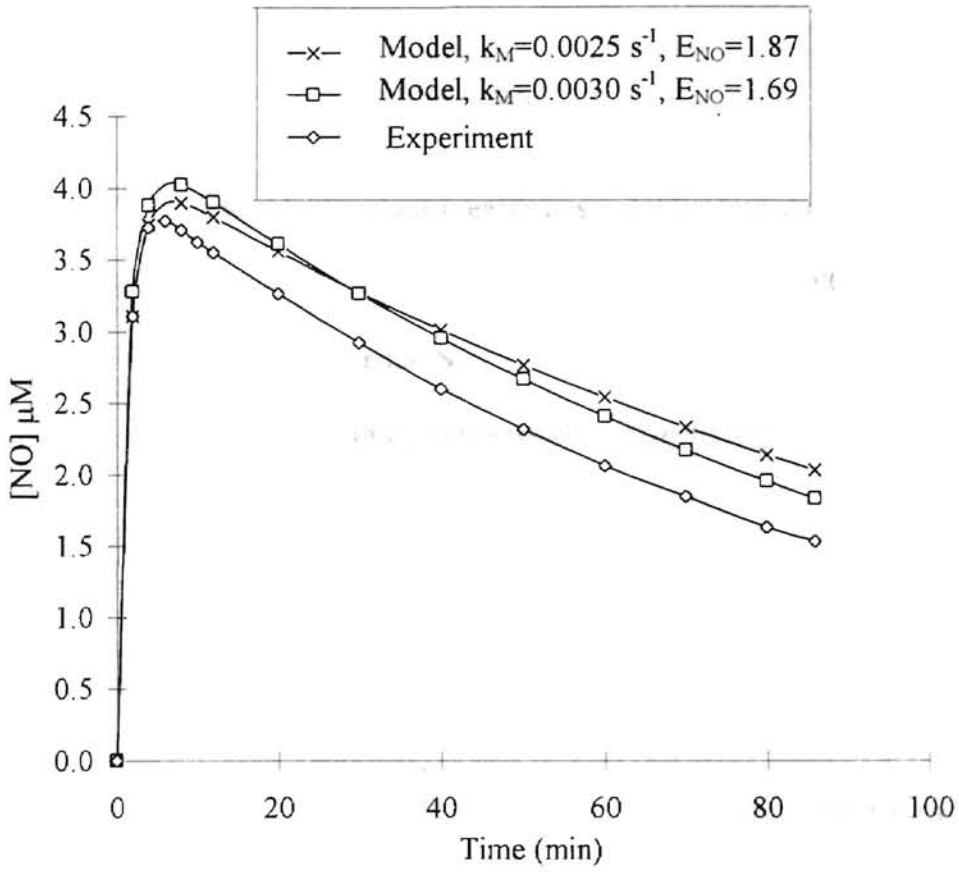

Figure 24. Effect of k_M on model predictions with Tyrode's buffer.

The slight disagreement of NO concentrations between model predictions and experiments could also possibly be due to NONOate injection quantities which vary slightly from predicted initial NONOate concentrations, or a minor error in the detector calibration.

5.4 Conclusions.

The following key results were obtained :

a) The model which includes reaction is capable of reliable predictions of NO concentrations generated by theoretical quantities of NONOates in oxygenated solutions. At high initial NONOate concentrations, the inclusion of the reaction of NO with O_2 in the model is essential for reliable predictions.

b) Better agreement of model predictions with experiments is observed at higher initial concentrations of NONOates. This is likely due to the minimization of errors in injecting the NONOate sample.

c) NO is not significantly depleted by reaction with species other than O_2 in culture media or Tyrode's albumin buffer. Therefore, these are suitable media for *in vitro* studies.

CHAPTER 6

CONCLUSIONS

A novel and convenient method was developed which enables accurate and reliable characterization of the kinetic parameters for NO release by NONOates. A major objective of this thesis was to improve upon previous methods for NONOate characterization. Spermine and Diethylamine NONOates, widely used in biomedical research, were characterized. Earlier studies (Maragos et al., 1991) did not measure aqueous NO directly. Further, the characterization procedure was such that E_{NO} could be determined for a species only after complete decomposition of the NONOate. This resulted in very long experiments and prevented the characterization of Spermine NONOate at physiological pH since the decomposition proceeded too slowly. Instead, the characterization of Spermine NONOate was carried out at pH 2, at which the NONOate decomposed faster. In addition, depletion of aqueous NO through mass transfer and reaction were not taken into account during NO analysis.

The current study detected aqueous NO directly by chemiluminescence. A modified ultrafiltration cell incorporating a semi-permeable membrane at its base provided a means by which NO from solution could be detected by chemiluminescence. Therefore, the requirement for complete NONOate decomposition was eliminated. Also, Spermine NONOate could be characterized at physiological pH within a two hour period. Depletion of aqueous NO via mass transfer was taken into account during the characterization. Reaction of NO in solution was minimized and hence neglected during NO analysis. An

added feature was that E_{NO} was determined over time. E_{NO} for Spermine NONOate was essentially constant throughout the entire experiment. However, for Diethylamine NONOate, an apparent initial burst of NO release was observed. This is a significant observation which merits further investigation. Knowledge of this is important in the design of applications where NONOates may be incorporated to deliver NO at controlled rates. The design of the experiment is general enough to be used to characterize other NO donors as well.

A major impact of the thesis was the development of a model which is capable of reliable predictions of NO concentrations following dissolution of theoretical amounts of Spermine NONOate. The model incorporated the kinetic parameters determined earlier by characterization. The requirement that E_{NO} remained constant allowed the model to be applied to NO generation by Spermine NONOate. The model took into account the depletion of NO through mass transfer and reaction with oxygen. The model was validated in oxygenated phosphate buffer, culture media, and Tyrode's albumin buffer. The model gave very good predictions in all three solutions, even at different initial NONOate concentrations. These results showed that no significant reaction of NO with species other than oxygen occurred in these solutions. In addition, the importance of including reaction of NO with O_2 in the model was demonstrated. Theoretical predictions of the NO concentrations obtained would be important in the design of NO delivery to targeted systems.

The salient feature of the model is its generality. Although the model has been applied to NO release by NONOates in a well stirred system, it can be used for other NO-donors

as well. Measurements of the NO concentration with time in the absence of reaction enables the evaluation of the NO-release rate for any NO-donor compound. Characterization of the NO-release rate using kinetic parameters can be incorporated into a model such as a well-stirred system or a plug flow reactor. Importantly, it is to be noted that the kinetic parameters used in characterizing NO release were determined in a different system (with rapid stirring and flow in the flow loop) from that in which a model predicting NO concentrations was validated (slow stirring, no flow loop). Yet, the ability of the model to make accurate and consistent NO concentration predictions in the latter system speaks for its generality of application.

6.1 Future studies.

The current study has brought out a few salient features of the NO releasing characteristics of Spermine and Diethylamine NONOates. While some of these are beyond the scope of this study, they are nevertheless important in making accurate estimations of NO released in aqueous solutions. One of the immediate concerns is the sensitivity of the k_M value to temperature. Although it is practically impossible to realize a perfectly insulated system, it would be a worthwhile effort to determine the k_M under thermostated conditions.

Another future line of work is the application of the model to make NO concentration predictions for donor species other than the NONOates, and check the validity of the model with experimental data. Having successfully characterized NO donors such as Spermine and Diethylamine NONOate, a suitable chemical delivery system incorporating

these NONOates, together with a reliable model, must be developed to deliver NO at desired rates to target systems. This is of great importance in therapeutic applications. As discussed in chapter 1, NO releasing drugs are used to counter effects of low endogenous NO levels, such as pulmonary hypertension. The NONOates may thus have to be encapsulated within a polymer coating or pellet. Studies in this area are already under progress. Smith et. al (1995) has studied NO-releasing polymers containing the [NO(NO)$^-$] group. Results proposed local delivery of NO using polymers containing NONOates as a viable alternative. However, Smith and co-workers only studied the time course of NO generation by random amounts of NONOates incorporated within a polymer sheath. In light of the observations made in this study, a future course of action is the study and modeling of the kinetics of NO release by defined amounts of NONOates incorporated in polymers. Also, it could be determined if the generated NO profile is affected by the presence of the polymer and to quantify any differences.

Finally, NONOates can also be used to study concentration dependent effects of NO on *in vitro* cell cultures and to estimate NONOate quantities necessary for NO delivery to targeted biological systems. Considering the number of physiological processes mediated by NO, NO donor compounds like NONOates offer good methods of NO delivery to counter a number of clinical problems.

REFERENCES

Archer, S., (1993) Measurement of nitric oxide in biological models. *FASEB.* **7,** 349-360.

Butler, A.R. and Williams, D.L.H. (1993) The physiological role of Nitric oxide. *Chem. Soc Rev*, 233-241.

Calver, A., Collier, J. and Vallance, P. (1993) Nitric oxide and cardiovascular control. *Exper. Phys.* **78**, 303-326.

Diodati, J.G, Quyyumi, A.A., Hussain, N. and Keefer, L.K. (1993) Complexes of nitric oxide with nucleophiles as agents for the controlled biological release of nitric oxide: Antiplatelet effect. Thromb-Haemost **70,** 654-658.

Diodati, J.G., Quyyumi, A.A. and Keefer, L.K. (1993) Complexes of nitric oxide with nucleophiles as agents for the controlled biological release of nitric oxide : Haemodynamic effect in the rabbit. *J. Card. Pharmacol.* **22**, 287-292.

Evans, C.H., Stefanovic-Racic, M., and Lancaster, J. (1995) Nitric oxide and its role in orthopedic disease. *Clinical Orthopedics and Related Research* No 312, 275-294.

Feelisch, M. (1991) The biochemical pathways of nitric oxide formation from nitrovasodilators · Appropriate choice of exogenous NO donors and aspects of preparation and handling of aqueous NO solutions. *J. Card. Pharmacol.* **17,** S25-S33.

Hogg, N., Darley-Usmar,V.M., Wilson, M.T., Moncada, S. (1992) Production of hydroxyl radicals from the simultaneous generation of superoxide and nitric oxide. *Biochem. J.* **281**, 419-421.

Ignarro, L.J. (1989) Endothelium-derived nitric oxide : actions and properties. *FASEB* **3**, 31-36.

Kerwin Jr., J.F., Lancaster Jr., J.R., and Feldman, P.L. (1995) Nitric oxide : A new paradigm for second messengers. *J. Med. Chem.* **38,** 4333-4362.

Lange, N.A. Lange's Handbook of Chemistry. rev. 10th edition (1967), McGraw Hill New York, N.Y, 1099-1101.

Lewis, R.S. and Deen, W.M., (1994) Kinetics of the reaction of nitric oxide with oxygen in aqueous solutions. *Chem. Res. Toxicol.* 7, 568-574.

Lewis, R.S., Tamir, S., Tannenbaum, S.R. and Deen, W.M. (1995) Kinetic analysis of the fate of nitric oxide synthesized by macrophages in vitro. *J. of Biol. Chem.* **270**, 29350-29355.

Luskove, J.A. and Frihman, W.H (1993) Nitric oxide donors in the treatment of cardiovascular and pulmonary diseases. *Am. Heart J.* **129,** 604-613.

Madison, D.V. (1993) Pass the nitric oxide. *Proc. Natl. Acad. Sci.* **90,** 4329-4331.

Maragos, C.M., Morley, D., Wink, D.A., Dunams, T.M., Saavedra, J.E, Holms, A., Bove, A.A., Isaac, L., Hrabie, J.A. and Keefer, L.K. (1991) Complexes of nitric oxide with nucleophiles as agents for the controlled biological release of nitric oxide. Vasorelaxant effects. *J. Med. Chem.* **34,** 3242-3247.

Moncada, S., Palmer, M.J. and Higgs, E.A. (1991) Nitric oxide : Physiology, Pathophysiology and Pharmacology. *Pharmacol. Rev.* **43**, 109-142.

Morley, D. amd Keefer, L.K. (1993) Nitric oxide /Nucleophiles complexes : A Unique class of nitric oxide-based vaodilators. *J. Card. Pharmacol.* **22**, S3-S9.

Moro, M.A., Darley-Usmar, V.M., Goodwin, D.A., Read, N.G., Zamora-Pino, R., Feelisch, M., Radomski, M.W. and Moncada, S. (1994) Paradoxical fate and biological action of peroxinitrite on human platelets. *Proc. Natl. Acad. Sci.* **91**, 6702-6706.

Smith, D.J., Chakravarthy, D., Pulfer, S., Simmons, M.L., Hrabie, J.A., Citro, M.L., Saavedra, J.E., Davies, K.M., Hutsell, T.C., Mooradian, D.L., Hanson, S.R. and Keefer, L.K. (1996) Nitric oxide-releasing polymers containing the [N(O)NO$^-$] group. *J. Med. Chem.* **39,** 1148-1156.

Snyder, S.H, and Bredt, D.S. (1992) Biological roles of nitric oxide. *Scientific American* **31**, 68-77.

Tamir, S., Lewis, R.S., de Rojas-Walker, T., Deen, W.M., Wishnok, J.S. and Tannenbaum, S.R. (1993) The influence of delivery rate on the chemistry and biological effects of nitric oxide. *Chem. Res. Toxicol.* **6**, 895-899.

Tannenbaum, S.R., Tamir, S., de Rojas-Walker, T. and Wishnok, J.S. (1991) DNA damage and cytotoxicity by nitric oxide. Proc. ACS Symposium on N-Nitroso compounds, Wash., DC.

Vallance, P. and Collier, J., (1994) Biology and clinical relevance of nitric oxide. *Br. Med. J.* **309**, 453-457.

APPENDIX A

MATHCAD SAMPLE PROGRAM

$k1 := 0.00025$ $\qquad O_2 := 0.87.\ 230$

$E := 1.87$ $\qquad k := 2.4\ .\ 10^{-6}$

$C := 82.7$

$K := 0.00168$

$y_0 := 0$

$D(x,y) := E.\ k1.\ (C).\ \exp(-k1.\ x) - K.\ y_0 - 4.\ k.\ y_0.y_0\ .\ O_2$

$Z :=$ rkfixed (y,0,6000,50,D)

$I := 0..\text{rows}(Z) - 1$

VITA

Candidate for the degree of

Master of Science

Thesis: CHARACTERIZATION AND MODELING OF NITRIC OXIDE RELEASE IN AQUEOUS SOLUTIONS

Major field: Chemical Engineering

Biographical:

Personal Data: Born in Bombay, India, On January 6, 1972, the son of Meenakshi and V.Ramamurthi.

Education: Graduated from Vidya Mandir, Madras, June 1990; received Bachelor of Engineering (Hons.) degree in Chemical Engineering from Bangalore University, Bangalore, India, August 1994; completed the requirement for a Master of Science degree at Oklahoma State University in December, 1996.

Experience: Intern at ICI (India) Ltd., Madras India, from December 1992 to February 1993. Graduate Research Assistant, Department of Chemical Engineering, Oklahoma State University, May 1995 to August 1995 and May 1996 to August 1996. Teaching Assistant, Department of Chemical Engineering, Oklahoma State University, August 1995 to May 1996.

Memberships: AIChE (Affiliate Member).